Mestrado Integrado em Engenharia Química

Production of Hydroxyapatite Nanoparticles for Cosmetic and Orthopaedic Applications: Effect of Chelants and Dispersants

Tese de Mestrado

desenvolvida no âmbito da disciplina de

Projecto de Desenvolvimento em Ambiente Empresarial

Daniela Filipa Moreira Correia

FLUIDINOVA
ENGENHARIA DE FLUIDOS

Universidade do Porto
Faculdade de Engenharia
FEUP

Departamento de Engenharia Química

Orientadores

Fluidinova - José Carlos Brito Lopes

FEUP - Madalena Maria Gomes de Queiroz Dias

Fevereiro de 2008

Acknowledgments

I would like to express my gratitude to my supervisors Professor José Carlos Brito Lopes and Professor Madalena Maria Gomes de Queiroz Dias whose expertise, understanding, and patience were constant. Although they are both very busy persons, they were always willing to take some time out from their busy schedule to enlighten any doubt I had.

I would also like to thank Viviana Manuela Tenedório Matos da Silva and Humberto Alexandre Beirão for the guidance and patience and without whom this work would not had been possible. From different ways, both provided me with direction, technical support and became my friends.

I would like to thank my friend, Marisa Rodrígues, for her daily help, essential to the concretization of this project. I must also acknowledge António Queimada for the availability for DSC analysis and Professor Joaquim Faria for letting me use his FT-IR.

Paulo Quadros for the support he provided at different levels of the research project and Paulo Gomes for his promptness to help me in any way possible.

My gratitude to all colleagues and friends in Fluidinova by their companionship and joy.

A special recognition to my parents for their love, motivation and encouragement.

Finally, I wish to thank my boyfriend, Luís, for his patience, understanding and support, in this moment of life transition.

To my parents

Abstract

In the present work, nanoparticles of hydroxyapatite (HAp) were obtained by wet chemical precipitation route from calcium/citrate/phosphate reactants at room temperature using the NETmix® technology. Parameters studied included: the maturation step; the influence of the amount of citrate added; and the effect of citrate anions on crystal growth. The surfactant (citrate) concentration during synthesis played an important role on the final properties of HAp nanoparticles.

The product was a transparent gel easily spread, of average particle size below 100 nm. Due to the presence of surfactant, HAp nanoparticles did not agglomerate or clump, like those without surfactant. Particles obtained were dispersed spheres, with high specific surface area (200-300 m^2/g). Samples were further analysed by X-Ray Diffraction, EDS, FT-IR and TG-DTA.

This product could be used as drug deliver in biomedical and cosmetic applications, since HAp are biocompatible nanoparticles with very high surface area.

Keywords: hydroxyapatite, wet chemical precipitation, surfactant, transparent gel.

Resumo

No presente trabalho, foram sintetizadas nanopartículas de hidroxiapatite (HAp) por precipitação química, via húmida recorrendo aos reagentes cálcio/citrato/fosfato à temperatura ambiente usando a tecnologia NETmix®. Foi estudada a influência da quantidade de citrato adicionado, a etapa de maturação e o efeito iónico do citrato no crescimento do cristal. A concentração de dispersante (citrato) teve grande influência nas propriedades finais das nanopartículas de HAp.

O produto obtido foi um gel transparente de fácil espalhamento, com um tamanho médio de partículas inferior a 100 nm. Devido à presença de dispersante, as nanopartículas de HAp não aglomeraram como as sintetizadas sem dispersante. As partículas do produto são esferas bem dispersas, com uma elevada área superficial (200-300 m^2/g). As amostras foram também analisadas por técnica de Difracção Raio-X, EDS, FT-IR and TG-DTA.

Atendendo à elevada área superficial e à sua biocompatibilidade, este produto tem um elevado potencial para a libertação controlada de fármacos em aplicações biomédicas e cosméticas.

Table of Contents

List of Tables

List of Figures

Notation

V	Ãdsorbed gas quantity,	m^3
V_m	Monolayer adsorbed gas quantity	m^3/mol
C	BET constant.	
P	Equilibrium pressure	
P_0	Saturation pressure of adsorbates at the temperature of adsorption	
E	Electron energy	ke-V
E0	Incident energy	ke-V
Z	Atomic number	
T	Temperature	ºC
Ksp	Constant of solubility product	
D	Crystallite size	Å
k	Shape factor equal to 0.9	
B	Diffraction peak width at half height	
b	Natural width of the instrument	
V_{esf}	Volume of a sphere	m^3
S_{esf}	Surface area of a sphere	m^2/g
V_p	Pores volume	cm^3/g
r_p	Particle radius	Å

Greek letters

ε	Solid porosity	
ε_p	Apparent porosity	
ρ_s	Solid density	g/m^3
ρ_{ap}	Apparent density	g/m^3
λ	X-ray wavelength (1.54060 Å)	Å
θ	Dffraction angle	º

List of Acronyms

SEM	Scanning Electron Microscopy
FT-IR	Fourier-Transform Infrared spectroscopy
BET	Brunauer, Emmett and Teller
XRD	X-Ray Diffraction
EDS	Energy Dispersive Spectroscopy
ICP-MS	Inductively Coupled Plasma Mass Spectrometry
TG-DTA	Thermogravimetric and Differential Thermal Analysis
DSC	Differential Scaning Calorimetry

1 Introduction

In recent years nanomaterials have been one of the centre focus of research groups and industry. Nanoscience and nanotechnology is an ever-growing multidisciplinary field of study attracting remarkable interest, investment and effort in research and development around the world. On the other hand, the demand of biocompatible materials is increasing substantially, representing an emerging worldwide market of several billion euros (Lu and Zhao).

Hydroxyapatite (HAp), a calcium phosphate, and the main component of bone, is one of these promising biomaterials that can act as bone or dental fillers, substitutes or replacements. Hydroxyapatite properties, such as bioactivity, biocompatibility, solubility, sinterability, fracture toughness and adsorption can be customized by phase composition and reaction control. Together with other nanostructure materials, it possesses unique surface, structural, and bulk properties that underline its important use in chemistry or pharmaceutical and biomedical fields. Therefore, HAp seems to be the most suitable ceramic material for hard tissue replacement implants and is probably the most widely studied bioceramic to date. It can also be used as the medium for column chromatography for protein separation, nucleic acids and virus, gas sensors, catalyst and host materials for lasers, as a bioimplant or as a drug deliverer. Nowadays, people are concerned with their health, well-being and physical appearance. There are also growing industrial and commercial interests in these matters. In the last decades, cosmetics have been attaining a considerable dimension. Hydroxyapatite is already used as skin filler, smoothing wrinkles, deep smile folds and scars. For example, Radiesse™ is a commercial form of injectable microspheres of hydroxyapatite in the form of gel for this same purpose. One of the advantages of this product when compared to other skin fillers is the long lasting results (years as oppose to a few months).

Natural bone, tooth enamel and skin cells all have a nanoscale structure, while many of the presently available forms of HAp are commercialized at a microscale. Comparing micrometric with nanometric HAp synthetic materials, a three order of magnitude difference in scale leads to better osteogenic and mechanical properties of the bone grafts, putties, prosthesis or implants based in nanoparticles of HAp. Hence, it has been the goal of many research works to develop methods for preparing HAp nanoparticles to substitute the microparticles in the current applications.

The main objective of this work was the development and characterization of a hydroxyapatite nanoparticle gel for topical administration.

1.1 Motivation and Relevance

Fluidinova, Engenharia de Fluidos, S.A. is a high technology engineering company. Fluidinova's core technologies are Computational Fluid Dynamics (CFD), chemical reactions for high intrinsic value products and fluid rheology. It has four main business areas: CFDapi – consulting services in industry, buildings and environment, using CFD; RIMCOP® – polymeric molding optimization by control of monomer injection and mixture; ROBpaint® – laboratory test equipment for painting inks; NETmix® – a novel static mixer.

NETmix® is used in Fluidinova's R&D unit as an optimized static mixer, which can be used to produce high value products, where mixing is one of the most important parameters to account for. Such products are nanomaterials, microemulsions and pharmaceutical compounds. With this technology, Fluidinova, in cooperation with INEB, Instituto de Engenharia Biomédica, has developed and patented an industrial process for the synthesis of high quality hydroxyapatite nanoparticles, commercialized under the name NanoXIM.

NanoXIM has extremely high purity and crystallinity and is to be used as biocompatible nanomaterial for biomedical and pharmaceutical applications. Fluidinova's main objective with NanoXIM is to improve the quality of the already existing hydroxyapatite based medical devices, such as bone grafts, coated implants and drug delivery systems (Fluidinova).

1.2 Thesis Objectives and Layout

This thesis was designed to study the effect of the incorporation of surfactants to diffuse hydroxyapatite nanoparticles, and characterization, to a final application in cosmetics.

The layout of the present work is divided as follows.

In Chapter 2 the state-of-the-art, an overview of the current knowledge on hydroxyapatite is presented. An intensive research was made on its properties, structure and synthesis methods present in literature. A study of the standard surfactants used to this end and at last, hydroxyapatite's wide applications.
In Chapter 3 a technical description on the experimental set-up and characterization procedures is made. In Chapter 4, all the results are presented and discussed. Finally, the general conclusions drawn from this work and some suggestions for future work modifications are presented in the Chapter 5.

2 State of Art

2.1 Introduction

Synthetic hydroxyapatite, HAp, is a calcium phosphate $Ca_{10}(PO_4)_6(OH)_2$, with composition similar to bone that has been attracting great attention and been widely used in different medical applications due to its exceptional biocompatibility and degree of bioactivity with human tissues.

Along with hydroxyapatite, there are many other kinds of calcium orthophosphates, listed inTable 1, and conventionally classified according to their Ca/P molar ratio, which varies from 0.5 to 2 (Gomes *et al.,* 2007).

Table 1. Calcium Orthophosphates: name, abbreviation, Ca/P molar ratio and chemical formula.

Name	Abbreviation	Ca/P molar ratio	Chemical Formula
Monocalcium Phosphate Monohydrate	MCPM	0.50	$Ca(H_2PO_4)_2 \cdot H_2O$
Dicalcium Phosphate Dihydrate	DCPD	1.00	$CaHPO_4 \cdot 2H_2O$
Dicalcium Phosphate Anhydrous	DCPA	1.00	$CaHPO_4$
Octacalcium Phosphate	OCP	1.33	$Ca_8H_2(PO_4)_6 \cdot 5H_2O$
Amorphous Calcium Phosphate	ACP	1.50	$Ca_3(PO_4)_2$
α-Tricalcium Phosphate	α-TCP	1.50	$\alpha - Ca_3(PO_4)_2$
β-Tricalcium Phosphate	β-TCP	1.50	$\beta - Ca_3(PO_4)_2$
Hydroxyapatite	HAp	1.67	$Ca_{10}(PO_4)_6(OH)_2$
TetraCalcium Phosphate	TTCP	2.00	$Ca_4(PO_4)_2O$

Calcium phosphates with a Ca/P molar ratio lower than 1.67 are referred as calcium-deficient hydroxyapatite (DHAp). It is believed that the Ca/P ratio influence the rate of hydrolysis and solubility of the bioceramic (Table 2) (Byrappa 2003). In general, the lower this ratio, the more acidic and soluble in water calcium phosphates are, because the apparent solubility of these phases is function of pH and calcium concentration.

Calcium-deficient hydroxyapatite is also represented by the chemical composition $Ca_{10-x}(HPO_4)_x(PO_4)_{6-x}(OH)_{2-x}$ where x ranges between 0 and 1, according to the stoichiometry. The most relevant orthophosphates are β-Tricalcium Phosphate, due to its bioresorbability, and hydroxyapatite due to its outstanding biocompatibility. Hydroxyapatite is more stable than tricalcium phosphates under physiological

conditions, since it has a lower solubility but TCP is rather soluble. However, many studies have indicated that the dissolution of HAp in the human body after implantation is too low to achieve the optimal results. On the other hand, the dissolution rate of β-TCP ceramics is too fast for bone bonding. To achieve an optimum resorbability of the material, studies have mainly focused on the biphasic calcium phosphate ceramics composed of HAp and TCP (Kwon *et al*., 2003).

Table 2. Calcium Orthophosphates: density, solubility and pH stability range in aqueous solution at 25ºC. Data compilation (Byrappa 2003; Dorozhkin and Epple 2002).

Compound	Density [g/cm^3]	Solubility at 25ºC, log(K_{sp})	pH stability range in aqueous solution at 25ºC
MCPM	2.23	1.14	0.0-2.0
DCPD	2.32	6.55	2.0-6.0
DCPA	2.89	6.9	[d]
OCP	2.61	49.6	5.5-7.0
ACP	-	[c]	[e]
α-TCP	2.86	25.5	[b]
β-TCP	3.07	28.9	[b]
HAp	3.16	58.5	9.5-12
TTCP	3.05	38.0	[b]

[b] These compounds cannot be precipitated from aqueous solutions. [c] Cannot be measured precisely. However, the following values were reported: 25.7 ± 0.1 (pH=7.40), 29.9 ± 0.1 (pH=6.00), 32.7 ± 0.1 (pH=5.28). [d] Stable at temperatures above 100ºC. [e] Always metastable. The composition of a precipitate depends on the solution pH value and composition.

2.2 Hydroxyapatite Applications

Calcium phosphates have been attracting great attention due to their biomedical applications and the absence of toxicity of their constituents. Many studies revealed the high affinity of hydroxyapatite with biopolymers such as proteins and enzymes; for that reason HAp is also used in high performance liquid chromatography (HPLC) for separating biological compounds (Dorozhkin and Epple 2002; Kandori *et al.*, 2002). HAp also finds applications in others fields of industrial or technological interest as catalyst or gas sensor or its possible use in water purification or manufacturing of biocompatible ceramics (Torrent-Burgues and Rodriguez-Clemente 2001). The major industrial application of calcium phosphate minerals is in the production of agricultural fertilizers.

Hydroxyapatite can also be used as a bioresorbable carrier material for controlled drug release, such as for the delivery of anti-tumor agents and antibodies in the treatment of bone infection such osteoporosis or osteomyelitis that is often treated by excision of necrotic tissue and irrigation of the wound. Hydroxyapatite has also being intensively referred and used in the treatment of other diseases such as diabetes.

Calcium phosphate ceramics are categorized as bioresorbable. Bioceramics became an accepted group of materials for medical applications, mainly for implants in orthopedics, maxillofacial surgery and for dental implants.

2.2.1 Orthopaedic and Dental Applications

For some time now, is known that hydroxyapatite is bioactive, since it has the same basic properties of human bones and teeth. It establishes a bond with the tissues, allowing the bone to grow and integrate the matrix, being used as bone graft or in coating of metallic implants, for orthopaedic, dental and maxillofacial applications, to facilitate the growth of bone and thereby raise the mechanical stability.

The medical community has accepted the bioceramics after a number of clinical tests. It has been known for more than twenty years that ceramics made of calcium phosphate salts can be used successfully for replacing and augmenting bone tissue (Thamaraiselvi and Rajeswari 2004).

To understand the difference between hydroxyapatite and bone mineral, there has been a considerable amount of research in this area. This difference lies mainly in the impurity content and crystallinity. Bone mineral is poorly crystalline apatite and contains different amounts of sodium, magnesium, water, and carbonate as major impurities, and zinc, strontium, aluminium, lead, and barium as minor impurities (Byrappa 2003; Dorozhkin and Epple 2002). This *carbonate hydroxyapatite* represents 65% of the total bone mass, with the remaining mass formed by organic matter and water. Most of this organic matter is collagen (Vallet-Regí and González-Calbet 2004) (*Table 3*).

Table 3. The composition of bone. Adapted from (Murugan and Ramakrishna 2005)

Inorganic phase	wt%	Organic phase	wt%
Hydroxyapatite	~60	Collagen	~20
Carbonate	~4	Water	~9
Citrate	~0.9	Non-collagenous proteins (osteocalcin, osteonectin, osteopontin, thrombospondin, morphogenetic proteins, sialoprotein, serum proteins)	~3
Sodium	~0.7		
Magnesium	~ 0.5		
Other traces: Cl^-, F^-, K^+ Sr^{2+}, Pb^{2+}, Zn^{2+}, Cu^{2+}, Fe^{2+}		Other traces: Polysaccharides, lipids, cytokines	
		Primary bone cells: osteoblasts, osteocytes, osteoclasts.	

According to Atsuo Ito and Kazuo Onuma (2), the *carbonate hydroxyapatite* promotes the differentiation of marrow stromal stem cells into osteoblasts that are boneproducing cells. Osteoblasts forms bone tissue on bioactive materials, finally bonding the material to the bone. Body fluid is highly supersaturated in HAp, and its deposition may occur on any biomaterial implanted in the body.

Collagenous proteins compose approximately 80 to 90% of the organic bone matrix. Regarding one early stage in the bone-bonding process, no collagen is observed in the organic matrix. Later, crystallites of HAp will grow in the organic matrix and an initial collagen fibber assembly is formed, mineralized, producing morphologically identifiable bone matrix. Bone regeneration rate depends on several factors such as porosity, composition, solubility and presence of certain elements that, released during the resorption of the ceramic material, facilitate the bone regeneration carried out by the osteoblasts.

Teeth exhibit similar characteristics to bones, except for their external surface coating, the enamel. Enamel has a much larger inorganic content than the bone (up to 90%,) and is formed by prismatic crystals, of larger dimensions which are strongly oriented. For this reason, their mechanical behaviour is different, since enamel is considered as the most resistant and tough material in the biological world. However, and in contrast with the bone, dental enamel in an adult body does not contain cells, and is therefore unable to regenerate itself; any deterioration that it may suffer becomes irreversible. Therefore, there is an evident need of remineralization of early dental lesions by deposition of HAp, so that can be incorporated into the dental structure at the point of lesion.

On the other hand, unwanted deposition of calcium phosphates in the body can lead to severe diseases. Calcium phosphates formation can be undesirable and avoided for biomaterials used in contact with blood, such as artificial blood vessels and artificial heart valves. This may result in calcification, thereby causing their mechanical failure and degradation and the use of surfactants is one strategy to prevent such calcification. It can also be a consequence of several diseases (atherosclerosis and dental calculus). Calcification is natural process of formation and growth of bone and teeth (in vivo crystallization of calcium phosphate), while dental caries and osteoporosis can be considered in vivo dissolution of calcium phosphates (Dorozhkin and Epple 2002).

2.2.2 Cosmetics

Recent applications comprise the use of hydroxyapatite in cosmetics and in esthetical treatments for diminishing wrinkles. Skin is the largest organ of the human body and the most visible. It is constituted by two layers. The top layer, the epidermis, serves to control the loss of water from cells and tissue. Without this protective barrier, the body would quickly dehydrate. Below the epidermis lies the second layer, the dermis, which is primarily made up of a protein called collagen (a biological polymer consisting of amino acids). This protein serves as a key structural component of connective tissue such as skin, bones, ligaments, etc. The dermis contains large amounts of collagen whose fibbers form a supporting mesh responsible for the skin's mechanical characteristics such as strength, texture and resilience.

As any material, collagen slowly breaks down over time. Skin cells called fibroblasts are capable of producing collagen, and when needed, fibroblasts replace broken collagen fibbers with new ones. As the years go by, the skin's ability to replace damaged collagen diminishes and more gaps and irregularities develop in the collagen mesh, leading to wrinkles. Thus, one important target of wrinkle prevention and elimination procedure is to reduce collagen breakdown and increase its supply. To reduce rather than just cover wrinkles, new collagen must become a part of the skin's inner layer, the dermis. Unfortunately, collagen molecules are too large to penetrate into the dermis when applied to the surface of the skin.

A common approach to smoothing wrinkles is collagen injections. This procedure does have some noticeable cosmetic effect but may have a number of serious drawbacks. Collagen for injections usually comes from animals sources and may be rejected, or may lead to a serious allergic reaction. Furthermore, the wrinkle smoothing effect of injections is relatively brief. Although injected collagen is trapped in the skin, it still fails to structurally integrate into the skin's own collagen mesh. As a result, it breaks down relatively quickly, which causes wrinkles to reappear. Another possibility is to extract a person's own collagen producing cells, grow them artificially and reinject in areas with wrinkles.

Hydroxyapatite particles can be used as skin filler. They may be delivered alone or in combination with other excipients. As was mentioned, skin’s aging shifts the balance between collagen production and breakdown leading to wrinkles, facial sag and rough skin texture. Stimulating skin cells to produce collagen can partly reverse this process. The benefit of stimulating the body own collagen production is that it stimulates collagen deposition in an orderly, structured manner and there is no risk of allergy, immune reaction or injection-induced infection. Due to its affinity for biopolymers as collagen, crystallites of HAp can grow in the dermis and an initial collagen fibber assembly formed, filling the wrinkle. Stimulation of collagen synthesis in aging skin is realistic and can substantially improve the appearance of fine lines and even deeper wrinkles when done correctly.

Due to its high surface area, HAp has the ability to incorporate a protein or a given drug, to retain it in a specific target site, and to deliver it progressively in time in the surrounding tissues (Byrappa 2003; Ginebra *et al*., 2006; Rauschmann *et al*., 2005). As (Bell 2006) relates, HAp core particles can be coated or impregnated at least

partially on the surface. This can be useful for aesthetical factors, intended to treat wrinkles, and/or skin imperfections. Moreover, it is possible to enhance skin elasticity, moisture, in the form of nutrients, vitamins or minerals, and/or improve appearance, treating other skin conditions as eczema, acne, rosacea, etc.

2.3 Hydroxyapatite Crystal

To understand HAp behaviour in a biological environment, a detailed knowledge of the chemical and physical properties of HAp is necessary.

Pure HAp crystallizes in the monoclinic space group $P_{21/b}$, but at temperatures above 250ºC, there is phase transition of hydroxyapatite from a monoclinic to a hexagonal system with a space group $P_{6\ 3/m}$, where each hexagon has three unit cells as is seen in Figure 1. According to Kay (1964)(referred for example by (Botelho 2005)), its crystallographic parameters are $a = 9.418\text{Å}$ and $c = 6.881\text{Å}$. Perpendicular to c-axis are three equivalent a-axes with a 120º angle between them.

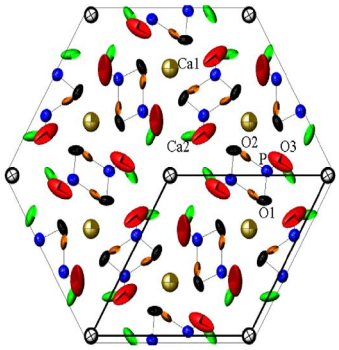

Figure 1. A c-axis projection for three unit cells of a synthetic HAp. Adapted (Leventouri 2006)

Hap's crystallographic structure consists of a closely packed arrangement of phosphate groups, which form two types of tunnels parallel to c axis, in which the Ca^{2+} ions are located. One of the main characteristics of apatites structure is to allow a large number of substitutions in its three sublattices, which leave the crystallographic structure unchanged (Vallet-Regía and González-Calbet 2004). The substitution of some calcium phosphates in the crystallographic structure by ions such as F^-, Na^+, K^+, Mg^{2+} and CO_3^{2-} can induce different properties. The existence of tunnels, in which the OH^- ions are located, gives the apatites certain properties close to those of zeolites. The tunnels can also accommodate small molecules such as H_2O.

The chemical formula of HAp can also be written as $Ca(1)_4Ca(2)_2(PO_4)_4(OH)_2$. The unit cell contains ten calcium atoms of which four calcium atoms occupy the $Ca(1)$ position and the other six calcium atoms occupy the $Ca(2)$ positions (Figure 2).

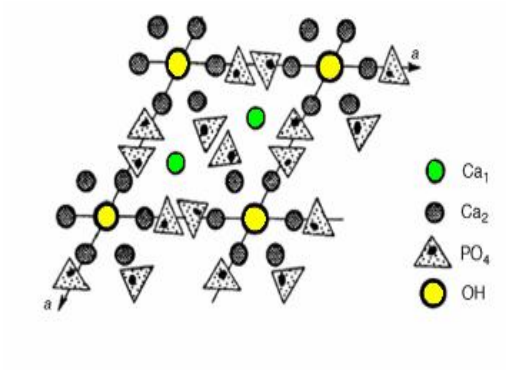

Figure 2 – Structure and typical morphology of hydroxyapatite (Sikirić and Füredi-Milhofer 2006)

The $Ca(1)$ atoms are aligned in columns (two at level $z=0$ and two at $z=1/2$) while the $Ca(2)$ atoms form an equilateral triangle perpendicular to c direction (one at $z=1/4$ and the other at $z=3/4$). The OH^- groups are at the corners of the unit cell and the six phosphates tetrahedral are positioned in a helical arrangement from level $z=1/4$ to $z=3/4$ (Figure 3).

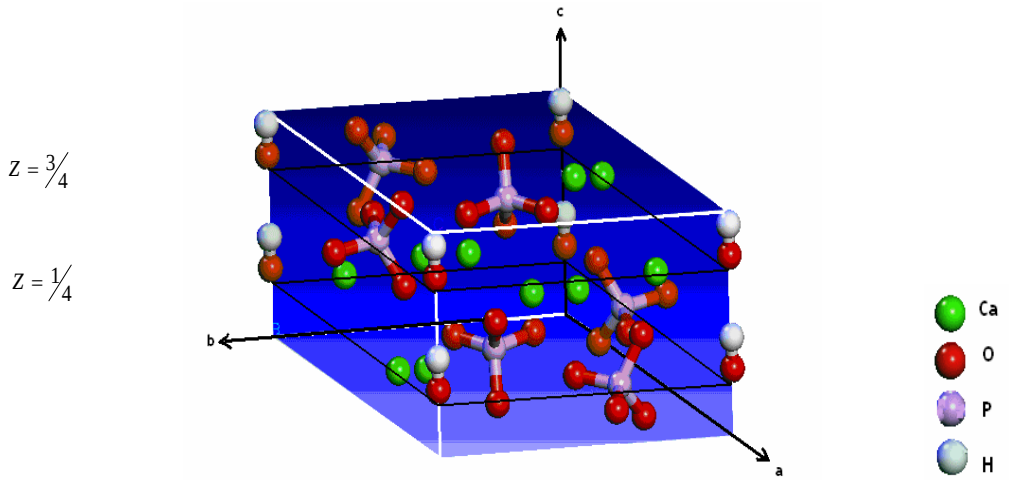

Figure 3. The structure of hydroxyapatite.

The phosphate groups are the basic skeletal framework that provides stability to the apatite structure (Byrappa 2003; Rangavittal *et al.*; Vallet-Regía and González-Calbet 2004). The bonds between the atoms P, $O1$, $O2$ and $O3$ of the phosphate tetrahedron have been drawn by (Leventouri 2006). Particle size and distribution are also relevant factors that determine the rheological properties of the suspensions and the packing ability of the powders both in suspension and in the green bodies (Rodríguez-Lorenzo *et al.*, 2001).

2.4 Hydroxyapatite Synthesis Methods

In the literature, various synthesis methods to prepare HAp are reported, mostly through solid-state reactions and wet chemical reactions (Koutsopoulos 2002), this last one being the most popular. These methods include different processing routes, some based on aqueous systems with inorganic reactant, such as hydrolysis of other calcium phosphate salts, crystal growth under hydrothermal conditions (Chen *et al*., 2004), sol-gel crystallization (Feng *et al*., 2005; Rodríguez-Lorenzo *et al*., 2001) and others as mechanochemical synthesis (Manuel et al., 2003) or ultrasonic spray freeze-drying (Itatani et al. 1999).

The method used in this study was the wet chemical route, via chemical precipitation. It is a process of great simplicity that requires low investment. This process allows highly controlled product properties such as morphology, size and reactivity. However, the composition, physicochemical properties, crystal size and morphology of synthetic apatites are extremely sensitive to preparative conditions and might result into non-stoichiometric calcium deficient HA powders. Usually, the formation of deficient hydroxyapatite is due to contaminations that come from reactant. This technique can be followed by additional processes, like filtering, washing and drying processes, and can include other steps such as micro-wave radiation treatments and/or aging (Gómez-Morales *et al*., (Byrappa 2003) 2001), addition of a solvent (sol-gel method), and wet chemically seeding immediately followed by drying with spray atomization (Byrappa 2003; Rodríguez-Lorenzo *et al*., 2001; Silva *et al*., 2008). However, it is not easy to obtain HAp nanoparticles powders, and recently a number of methods to form apatite nanoparticles at ambient temperature have been introduced. Among these methods, in situ formation of composites nanoparticles of hydroxyapatite by forming HAp crystals through the presence of active groups such as chelate is one of the attractive routes (Li et al. 2007a).

The final application of the Hap powders conditions important properties such as purity, degree of crystallinity, crystal and average particle size, heavy metal contamination, specific surface area, porosity and pore size distribution.

2.5 NETmix® Reactor

HAp nanoparticles were produced using the NETmix® technology, a new type of static mixing device for continuous mode operation (Laranjeira 2005). With a structural network arrangement of spherical chambers connected by cylindrical channels (Figure 4), it promotes strong mixing dynamics enabling spatial control of micromixture quality (Figure 5).

This regulates the mixing phenomena at the molecular level, the scale at which reactions occur. Other mixers, static or traditional stirred tanks are not as effective, since mixing is generally only effective at the macromixing scale. The micromixing characteristics of the NETmix® represent a key factor to determine HAp properties, such

as purity, crystallinity, particle size distribution, crystallites size and morphology (Gomes *et al*., 2007; Silva et al. 2008)

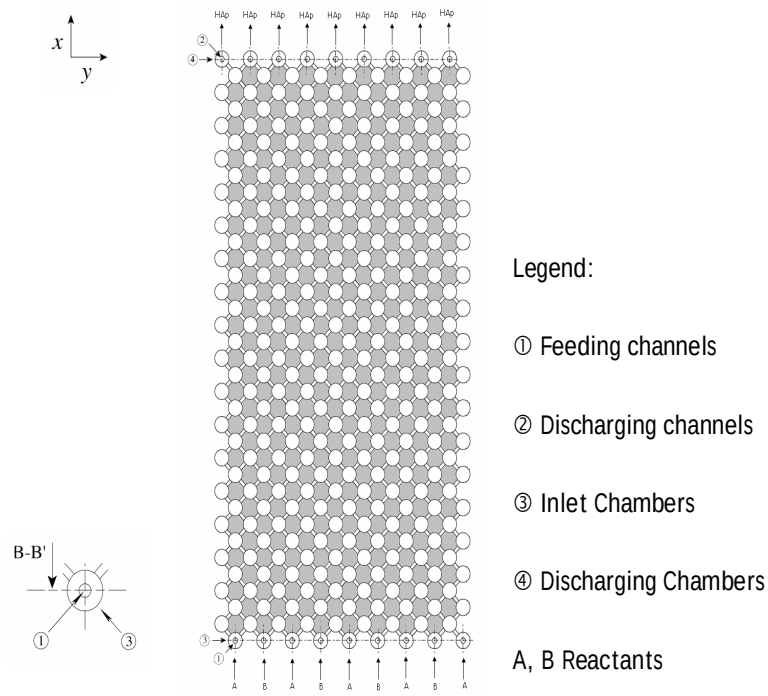

Figure 4. NETMIX® static mixer schematic representation, adapted from (Laranjeira 2005).

The NETmix® static mixer represents an industrial advantage, since due to its simple structure and the possibility of different injection schemes, the scale-up of this process is immediate by associating several NETmix® static mixers in parallel or in series. Easily adaptable, it can be constructed in different materials, sustaining temperature, pressure and concentration control and reaction selectivity without modifying its dynamics. It has the ability to control the mean residence time of the reactants, mixing intensity and scale. With a large heat exchange area it ensures temperature control for highly endothermic or exothermic reactions.

This technology was successfully applied for the synthesis of HAp nanoparticles with high reproducibility, mainly in terms of size distribution. The process, based on wet chemical precipitation was patented by Fluidinova and INEB, Instituto Nacional de Engenharia Biomédica.

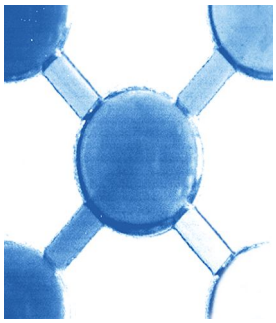

Figure 5. Structural network arrangement of spherical chambers connected by cylindrical channels. Adapted from (Laranjeira 2005)

2.6 Surfactant Agent

Most of the usual forms of HAp are microstructures and the use of surfactants combined with the right synthesis method enables the production of nanostructures of HAp. These nanostructures are closer to those occurring in natural HAp in bone and tooth enamel, leading to better osteogenic and mechanical properties of the bone grafts, prosthesis or implants (Balasundaramm and Webster 2006; Chan et al. 2006) literature reports the use of amino acids, proteins, and carboxylic acids as HAp crystal growth inhibitors (Amjad 1987). Surfactants have been used in all three anionic, cationic and non-ionic groups.

(Wu and Bose 2005) used mono-dodecyl phosphate as surfactant, and claimed that HAp nanopowders synthesized with this surfactant showed better densification ability as they had higher surface area. (Pradeesh et al. 2005) prepared microspheres of hydroxyapatite of definite size with sphere in sphere morphology and used three different stabilizers: Tween-40, sodium laurate and poly-vinyl-alcohol (PVA). Only PVA gave regular spherical spheres while others gave irregular shaped agglomerates. Cetyltrimethylammonium bromide (CTAB) is a cationic surfactant, commonly used in hydroxyapatite synthesis (Li et al. 2007b; Wang et al. 2006; Yao et al. 2003). (Chen et al. 2004) used a nonionic biodegradable surfactant, Tomadol 23–6.5, that allows to control nucleation and growth, minimizing the degree of agglomeration, producing HAp with high chemical purity.

In this work, potassium citrate was chosen as the surfactant (Figure 6), since it is a minor bone component, and thus it is not rejected. Yet, the interaction mechanism between citrate and HAp is not clearly understood. Among authors there are still differences of opinion. Misra (1996) states that there is an ion-exchange mechanism between citrate and phosphate ions at the HAp surface, while López-Macipe et al. 1998 propose that adsorption takes place by interaction between citrate and the adsorption sites at the HAp surface. For the calculations in this work, the second mechanism was considered. To estimate the amount of surfactant that is adsorbed in a monolayer, it was considered that crystals of HAp join together to form a cluster of 40nm, with a total of 11 112 external calcium atoms exposed. Each calcium atom adsorbs one citrate ion (cit^{3-}), according to the mechanism described in López-Macipe et al. 1998. Detailed calculations are given in Appendix A.

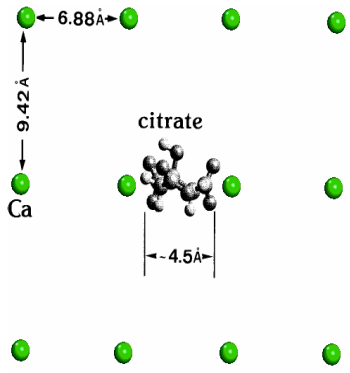

Figure 6 – Outline of the adsorption of the –COO⁻ groups of Cit^{3-} on the (100) face of the hydroxyapatite (HAp) crystal, from CERIUS² Molecular Simulations Inc. Adapted from (López-Macipe et al. 1998)

When Ca^{2+} is present in excess in the bulk solution, calcium citrate, ($Ca_3(C_6H_5O_7)_2 \cdot 4H_2O$), rapidly forms and precipitates (López-Macipe et al. 1998; Martins et al. 2008; Misra 1996).

3 Technical Description

3.1 Experimental Set-up

The NETmix® reactor (Figure 7), used in this work, is a small NETmix® unit made of Teflon with total volume of 50ml with a thermostatic jacket and 9 inlet/outlet ports. The reactants are fed to the reactor through two pumps connected to the correspondent distributors, which are programmed according to the desired injection scheme. The outlets are connected to a collector that discharges the final product in the recipient.

Legend:
1 – NETmix® Reactor
2 – Distributors
3 – Collector
4 – Pumps
5 – Reactor vessels
6 – Thermostatic bath.

Figure 7. Pharma·NETmix® Reactor laboratorial set-up

Distilled water and analytical reagent chemicals were used for the preparation of the reactant solutions. Calcium dichloride ($CaCl_2$) (97% Sigma) with potassium citrate ($K_3(C_6H_5O_7)_2$) 99.5% of purity and potassium dihydrogen phosphate 99% purity (KH_2PO_4) were prepared from the respective extra pure solids (Riedel-de Haën). Potassium hydroxide solution was prepared from concentrated standard 85.0% of purity (Riedel-de Haën). The precipitation reaction for HAp production is described as follows (Lopes et al. 2006):

$$10Ca_{(aq.)} + 6PO_{4(aq.)} \xrightarrow{OH^-} Ca_{10}(PO_4)_6(OH)_{2(s)} \quad (1)$$

To produce Hap by the wet chemical precipitation method two different reactant solutions were used: reactant A, a solution of $CaCl_2$ and potassium citrate, thoroughly mixed; and reactant B, a solution of KH_2PO_4 and KOH. Each solution was pre-mixed and fed separately, according to the injection scheme of Figure 8.

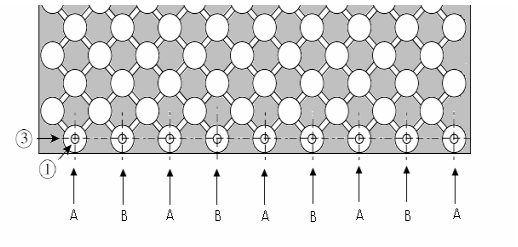

Legend:

① Feeding Channels

③ Inlet Chambers

A, B Reactants

Figure 8. Pharma·NETmix® Reactor – Injection scheme.

In the series of experiments done, Citrate to Calcium, Cit/Ca ratio in reactant A ranged from $1x10^{-3}$ to 1.87. Most of the experiments were performed at room temperature and in order to study the effect of temperature, one experiment was performed at 50ºC. In this case, reactants were kept in a thermostatic bath at constant temperature and the thermostatic jacket was filled with water at 50ºC.

The final product was a suspension that was subjected to a maturation stage at different aging times. The evolution of particle size distribution, and BET area were controlled. To obtain dry powder, the suspension was centrifuged, washed with distilled water (Appendix B), until no chlorine and potassium ions were detected after rinsing. It was milled (Appendix C) and dried at 60ºC, for chemical and physical characterization.

3.2 Characterization

From the series of fourteen experiences made, only C01 and C02 samples were chosen to be completely characterized. C013 experiment had the purpose to test the reproducibility of C01. The N24 experience is a formulation identical to C01 and C02, without surfactant (Table 4).

Table 4. Samples with different Cit/Ca ratio (α).

Sample	Ratio Cit/Ca
C01	α
C02	0.2α
C13	α
N24	-

3.2.1 Distribution of particle size

To characterize the distribution of particle size and morphology of HAp nanoparticles, both the original suspensions and the powders were analysed with light scattering using a MALVERN Hydro 2000S, with a lower detection limit of 20 nm. Malvern uses Mie theory (Mastersizer2000 2007) to predict light scattering behaviour, knowing specific information, such as the refractive index (1.6) and absorption. It works by using the optical

bench to capture the actual scattering pattern from a field of particles. Then, using Mie theory for spherical particles, it calculates the size particles that created that pattern.

3.2.2 Scanning Electron Microscopy (SEM)

SEM is one of the diffraction electron technique which was used to observe the microstructure of hydroxyapatite. The image is formed by scanning point-to-point the sample surface with an electron beam of high energy and the detectors collect the signal emitted by the sample surface and the intensity of the detected signal and producing high-resolution images of the sample surface.

The equipment used for the analysis is a Hitachi S-4100, Japan, Vacc = 25 kV. The samples analysed through this technique were in powder, suspensions and powder in ethanol solution.

Powder samples were prepared by fixing the powder in a double-side adhesive conductive carbon tape glued in a metallic sample holder. An original suspension sample was vigorously shaken before adding two drops on the surface of a microscopic glass after that, the glass was glued on the carbon tape. The same treatment was made with the sample suspended in ethanol. Finally, all the samples above have had a carbon film deposition through evaporation before been analysed.

Energy Dispersive Spectroscopy (EDS)

EDS consist on a primary beam of electrons that is scattered at high angles (>90º) and reach the sample surface with high energy (>50 eV). Rutherford equation for elastic scattering correlates for a given incident radiation, E0, the scattering angle increase with the atomic number of the sample.

$$\Omega(>\theta) = 1.62 \times 10^{-20} \frac{Z^2}{E^2} \cot^2 \frac{\theta}{2} \left[cm^2\right] \qquad (2)$$

Cross section Ω, $(>\theta)$ represents the probability of elastic scattering with change of electron direction bigger than θ, Z the atomic number and E the electron energy [keV].

The sample is prepared the same way as for SEM. The instrument model is a Bruker AXS Microanalysis GmbH, Germany.

3.2.3 X-Ray Diffraction (XRD)

X-Ray Diffraction technique was used to identify unknown crystallized substances, by comparing diffraction patterns with a database. To observe the components in the powder and assess HAp crystalline phases, samples were exposed to Cu Kα radiation (40 kV and 50 mA) in a wide angle X-ray diffractometer (λ = 1.54060 Å) (model

Philips X'pert mod. MPD, Netherland). The instrument was operated in the step-scan increments of 0.05º 2θ/s and diffraction angles between 5º <2θ <60º.

3.2.4 Differential Scanning Calorimetry and Thermogravimetric and Differential Thermal Analysis

Differential Scanning Calorimetry (DSC) is one of the most frequently used techniques in the field of thermal characterization of solids and liquids. The DSC method can be used for the analysis of energetic effects such as: melting/crystallization behaviour, solid-solid transitions, polymorphism, degree of crystallinity, glass transitions, cross-linking reactions, oxidative stability, decomposition behaviour, purity determination, specific heat.
Applying this technique, a sample is placed inside a crucible which is then placed inside the measurement cell (furnace) of the DSC system along with a reference pan which is normally empty. By applying a controlled temperature program (isothermal, heating or cooling at constant rates), caloric changes can be characterized (Netzsch).

Differential scanning calorimeter (DSC) analyses were performed on a NETZSCH DSC 200 F3. The The samples to be analysed (3-5mg) by DSC were crimped non hermetically in an aluminium pan and heated from 30ºC to 450ºC at a rate of 10ºC/min under nitrogen purge. Thermogravimetric and Differential Thermal Analysis (TG/DTA) were performed on a NETZSCH model STA 409 EP. This analysis (DTA) is very similar to DSC, but DTA complements it by determining changes in weight in relation to change in temperature. DTA samples were heated from 25ºC to 1300ºC at a rate of 10ºC/min.

3.2.5 Fourier-Transform Infrared spectroscopy (FT-IR)

Fourier transform spectroscopy is a measurement technique based on the fact that molecules have specific frequencies at which they rotate or vibrate corresponding to discrete energy levels. The infrared spectrum of a sample is collected by passing a beam of infrared light through the sample. Examination of the transmitted light reveals how much energy was absorbed at each wavelength. A Fourier transform instrument measures all wavelengths at once. From this, a transmittance or absorbance spectrum can be produced, showing at which IR wavelengths the sample absorbs. Analysis of these absorption characteristics reveals details about the molecular structure of the sample.

For FTIR, the gel was dried and dispersed into pellets of KBr and the spectra obtained in a Bomem-Grams/386 (4 cm^{-1} of resolution) in the range of 400 to 4000 cm^{-1}.

3.2.6 Specific Surface Area measurement (SSA)

Specific surface area measurement technique was performed in this study. Samples were pre-treated, before performing gas sorption, to eliminate contaminants such as water and oils through degassing treatment which is

basically pre-heat the sample in a vacuum environment for a number of hours and temperature defined by the sample matrix.

Small amounts of a nitrogen gas (the adsorbate) are admitted in steps into the vaccum sample chamber. Gas molecules that are adsorved on the surface of the solid-sample (adsorbent) tend to form a thin layer that covers the entire adsorbent surface (Langmuir theory). Based on the well-known Brunauer, Emmett and Teller (BET) theory, one can estimate the quantity of molecules required to cover the adsorbent surface with a monolayer of adsorbed molecules. Continued addition of gas molecules beyond monolayer formation leads to the gradual stacking of multiple layers (or multilayers)(Quantachrom).

$$\frac{V}{V_m} = \frac{C(P/P_0)}{(1-(P/P_0))(1-P/P_0+C(P/P_0))} \tag{3}$$

V is the adsorbed gas quantity, and V_m is the monolayer adsorbed gas quantity. *P* and P_0 are the equilibrium and the saturation pressure of adsorbates at the temperature of adsorption and *C* is the BET constant.

Specific surface areas of powders (SSA) were determined with a BET Surface Area Analyser (Quantachrom Nova 2000e, with sample degasification temperature of 200ºC in 2h, 5 point analysis and equilibrium time of 130 s).

4 Results and Discussion

HAp suspensions were aged for periods between one hour to thirty days. During this period, crystals were subjected to a recrystallization process. No dissolution signs were detected, since the pH was approximately constant around 12. N24 sample (Figure 9a) has no surfactant and a permanent two phase state suspension is clearly observed. On the other hand, C01 sample has the same phase separation in the first days (Figure 9b) which disappeared as the maturation process went through, turning the white suspension into a bluish transparent liquid (Figure 9c). In this case, the maturation stage helps crystals in suspension to balance the ionic charges that can promote agglomeration and diffuse. It was observed that temperature accelerates the process, since approximately the same particle size distribution of C01 is obtained in fewer days. This maturation stage was interrupted at different times, followed by a washing process (Appendix B). A transparent gel was obtained and the sample was then wet milled (Appendix C) in a planetary ball mill equipment and finally dried (Figure 10).

If the suspension is not properly washed, chloride ions $(r_{Cl^-} = 181 ppm)$ may enter the crystal lattice of HAP substituting hydroxyl groups $(r_{OH^-} = 151 ppm)$ through temperature. Reports relate that potassium ions can substitute calcium ions into the HAP crystal lattice and form locally nonstoichiometric HAP in the bulk crystal, although this rises some doubts due to the different charges and the significant difference in the radius of the two ions $(r_{Ca^{2+}} = 99 ppm, r_{K^+} = 133 ppm)$ (Koutsopoulos 2002).

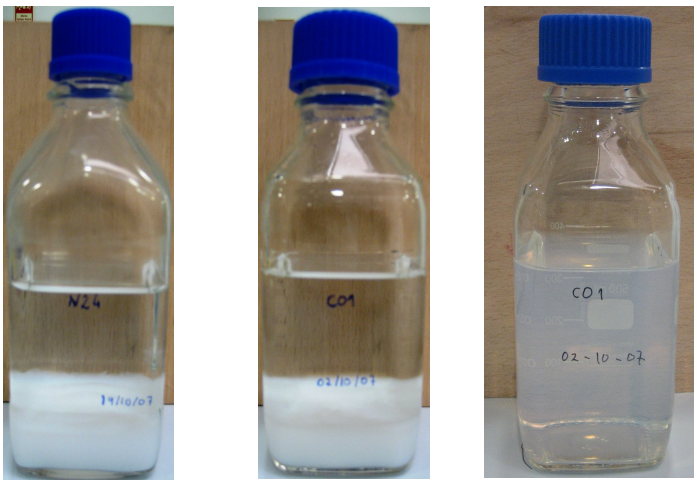

a) b) c)

Figure 9. Suspensions of hydroxyapatite: a) without surfactant; b) with surfactant, without maturation; b) with surfactant, 4 days maturation.

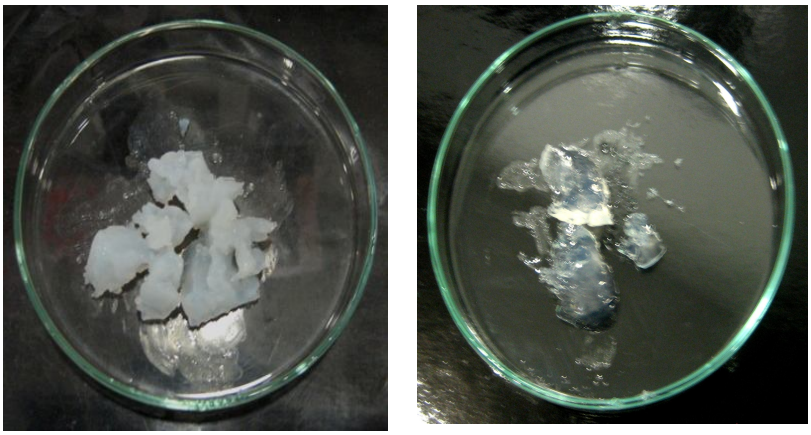

a) b)

Figure 10.Hydroxyapatite: a) N24 sample, white precipitated; b) C01 sample, transparent gel.

4.1 Particle Size Distribution and Crystals Morphology

For the particle size distributions an operation protocol was developed for suspensions and powders analysis, and a study of the effect of maturation time was observed. The original suspensions of samples C01, C02 and N24 were analyzed at 1 hour, 24 hour, 4, 7 and 30 days, as shown in Table 5.

Table 5. Population distribution of samples C01, C02 and N24 with different maturation times.

		Distribution (µm)		
Sample	**Maturation Time**	**d(0,1)**	**d(0,5)**	**d(0,9)**
C01	1h	4.471	12.802	26.963
	24h	7.409	18.759	40.238
	4 days	0.070	0.100	0.149
	7 days	0.071	0.101	0.150
	30 days	0.068	0.096	0.146
C02	1h	5.666	10.553	19.099
	24h	4.879	9.905	18.773
	4 days	4.838	9.739	19.469
	7 days	2.266	5.531	29.241
	23 days	0.071	0.102	0.152
N24	1h	6.405	12.175	22.159
	24h	4.193	7.970	14.521
	4 days (US)	0.077	0.115	0.170
	4dyas (no US)	5.444	13.460	48.535

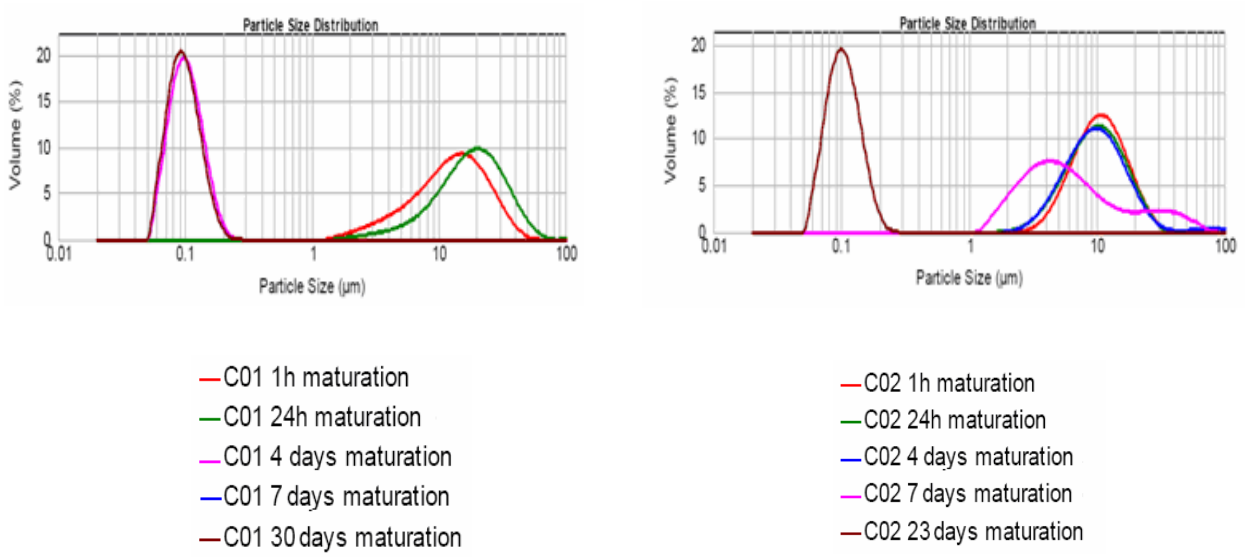

a) *b)*

Figure 11. Particle size distribution of original suspensions along maturation a) Sample C01, b) Sample C02.

With time, a decrease on the particles size distribution is observed. For sample C01 at the end of 4 days, 50% of the particles distribution is below 100 nm and 90% is below 149 nm (Figure 11a). Sample C02 reaches similar values after 23 days with 90% of the population below the 152 nm (Figure 11b).

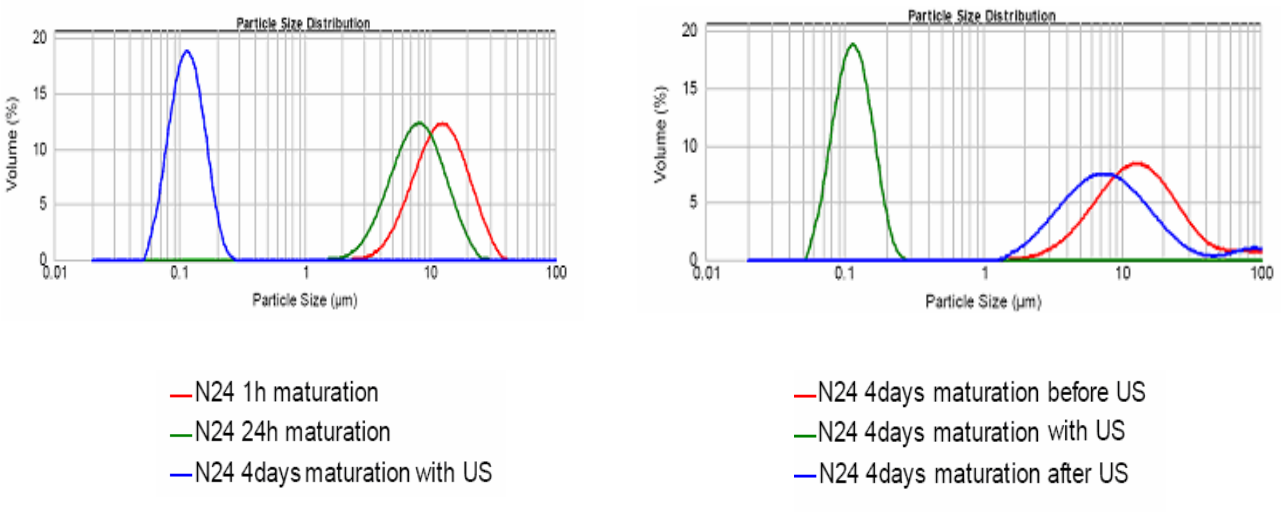

a) *b)*

Figure 12. Particle size distribution of original suspensions a) Sample N24 along maturation, b) Sample N24 with different ultra-sound dosages.

Although sample N24 achieve 50% of population with 115 nm at the end of 4 days (Figure 12a), due to its strong agglomeration state, high dosage of ultra-sound was needed to obtain a particle size distribution close to the surfactant samples. However, as time passes within each measurement, it reveals that the suspension was not stable and re-agglomerated (Figure 12b) after a short period of time. The stability of samples C01 and C02 seems to be due to the presence of citrate, by leading to the formation of micelles around each particle, controlling its growth and agglomeration prevention.

These results are confirmed by SEM micrographs which give detailed information of the samples microstructure. Observing Figure 13 from a) to e), particles morphology is clear: spherical shape and a homogeneous distribution with an average particle size around 50nm. In the image f), small particles are visible, strongly agglomerated, due to the lack of a surfactant.

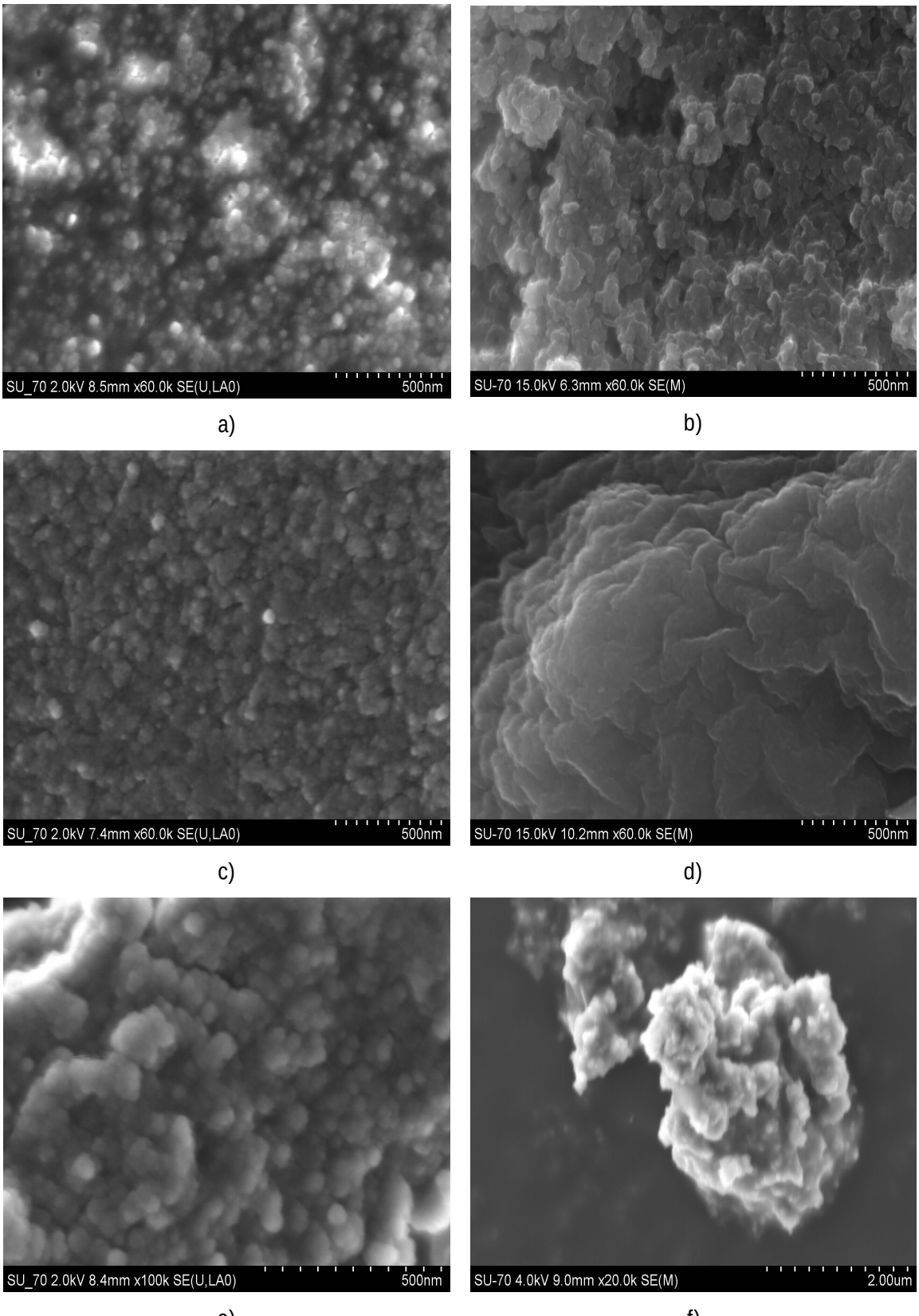

Figure 13. SEM images of samples: (a) C01 in the form of suspension (scale 500 nm), (c) C01 dry washed gel (scale 500nm) and (e) C01 powder dissolved in ethanol (scale 500 nm); (b) C02 in the form of powder (scale 500 nm), (d) C02 dry washed gel (scale 500nm), (f) N24 in the form of powder (scale 2.00 µm)

.

4.2 Elemental Analysis

With EDS (energy dispersive spectroscopy), a qualitative elemental analysis was done, to determine which elements are present and their relative abundance. A SEM micrograph of a gel from sample C02 was used, revealing a blurry image, and no particles were distinguished because it is in a gel form state (Figure 14 a).

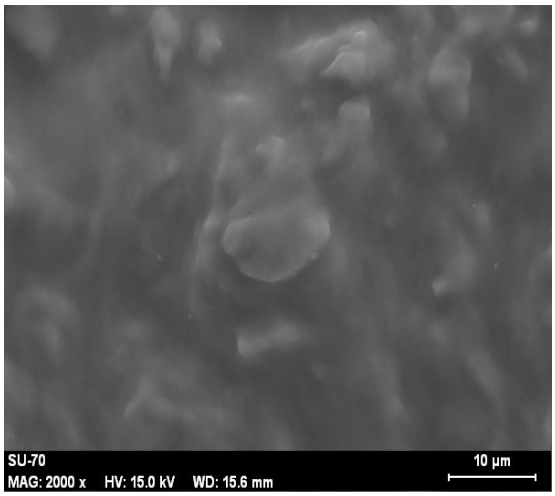

a)

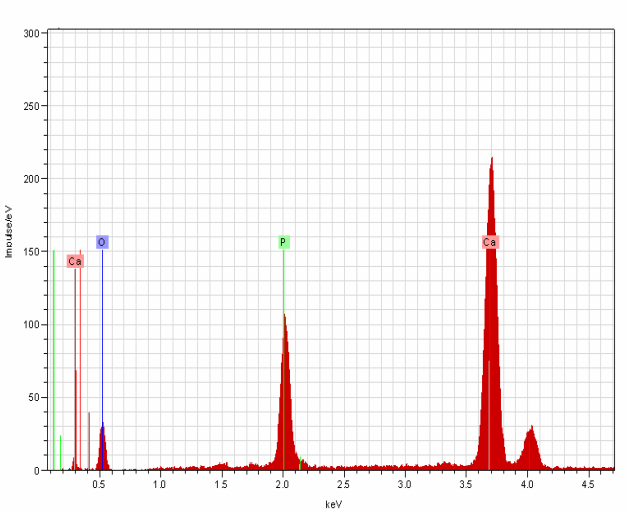

b)

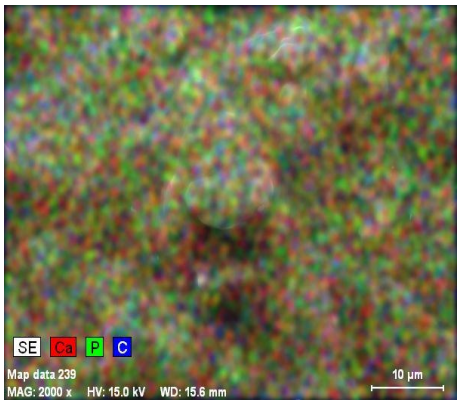

c) All elements

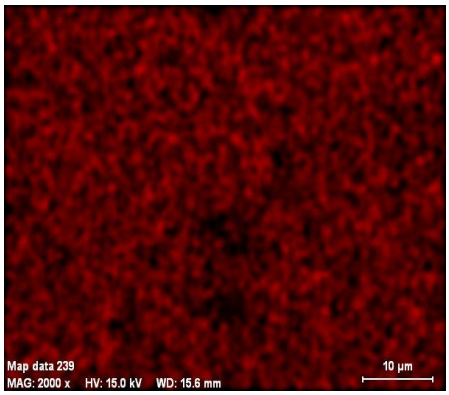

d) Calcium

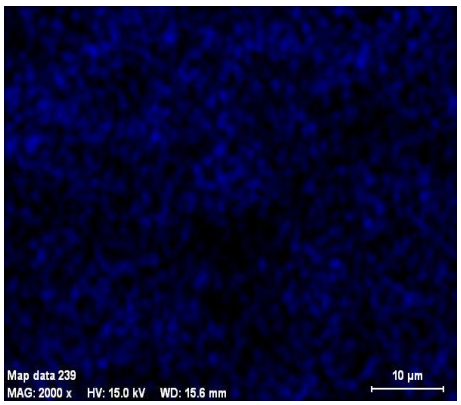

e) Carbon

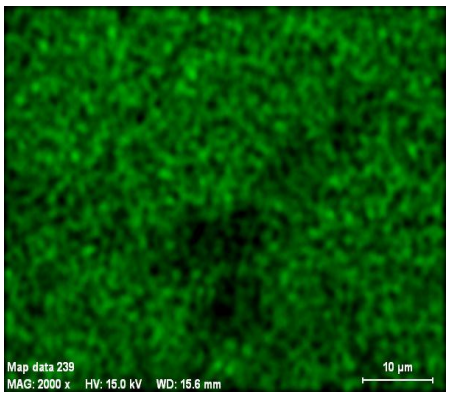

f) Phosphorus

Figure 14. Gel sample from C02. a) SEM micrograph; b) EDS analysis; c) EDS analysis with all elements identified; d) Calcium element; e) carbon element; f) phosphorus element.

In Figure 14b it is possible to observe the identified elements, calcium, phosphorus, carbon and oxygen. Carbon comes from COO^- group so as part of the oxygen, present in the sample. In Figure 14c it is possible to observe the equal distribution of the elements on the surface, and detailed in Figure 14 d, e and f. The distribution is homogeneous, appearing that hydroxyapatite nanoparticles are well dispersed. The identified elements are written in Table 6. The amount of carbon is approximately zero, because carbon and calcium were overlapping and in the calculation, the peak is all attributed to calcium.

Table 6. Percentage of each element present in sample C02.

Element	Norm. Conc. [norm. wt.-%]	Atom Conc. [norm. at.-%]	Error %
Calcium	55.67	41.15	1.850
Phosphorus	25.97	24.84	1.150
Oxygen	18.37	34.01	3.910
Carbon	~0	~0	0.025

Note that no other contaminant elements were detected through this method, verifying the quality of the reactants used in HAp synthesis. *Table 7* shows the minimum trace of heavy metal content that where found in N24 sample through ICP-MS method.

Table 7.Trace element concentrations of heavy metals for ASTM Standard F1185-88 and sample N24.

Element (ppm)	As	Hg	Cd	Pb
ASTM Standard F1185-88	*< 3*	*< 5*	*< 5*	*< 30*
N24	N/A	< 0.037	0.26	1.1

4.3 Presence of Crystalline Phases

In *Figure 15* diffractograms of HAp with (C01) and without (N24) surfactant are shown. C01 and N24, green and pre-heat treated. Comparing both green (without pre-heat treatment) samples, it is clear the presence of HAp in both samples. The emitted radiation is scattered in many directions, for C01 nanoparticles there is great background noise. C01 was under a high temperature XRD analysis (from room temperature to 800ºC) in order to investigate the appearance of other elements. In fact, the HAp's characteristic peak of $2\theta = 32º$ suffered a loss of intensity and other three appeared at $2\theta = 39º$ e 46º and 67º. This phenomenon requires further analysis (see future work) to investigate the thermo-kinetic applied in order to understand its mechanism. However due to the absence of any evidence of other elements in the sample, no conclusion can be made. As calcium citrate peaks overlap with Hap ones, the XRD analysis report clearly states that only hydroxyapatite (JCPDS 010-6309) is present in the sample.

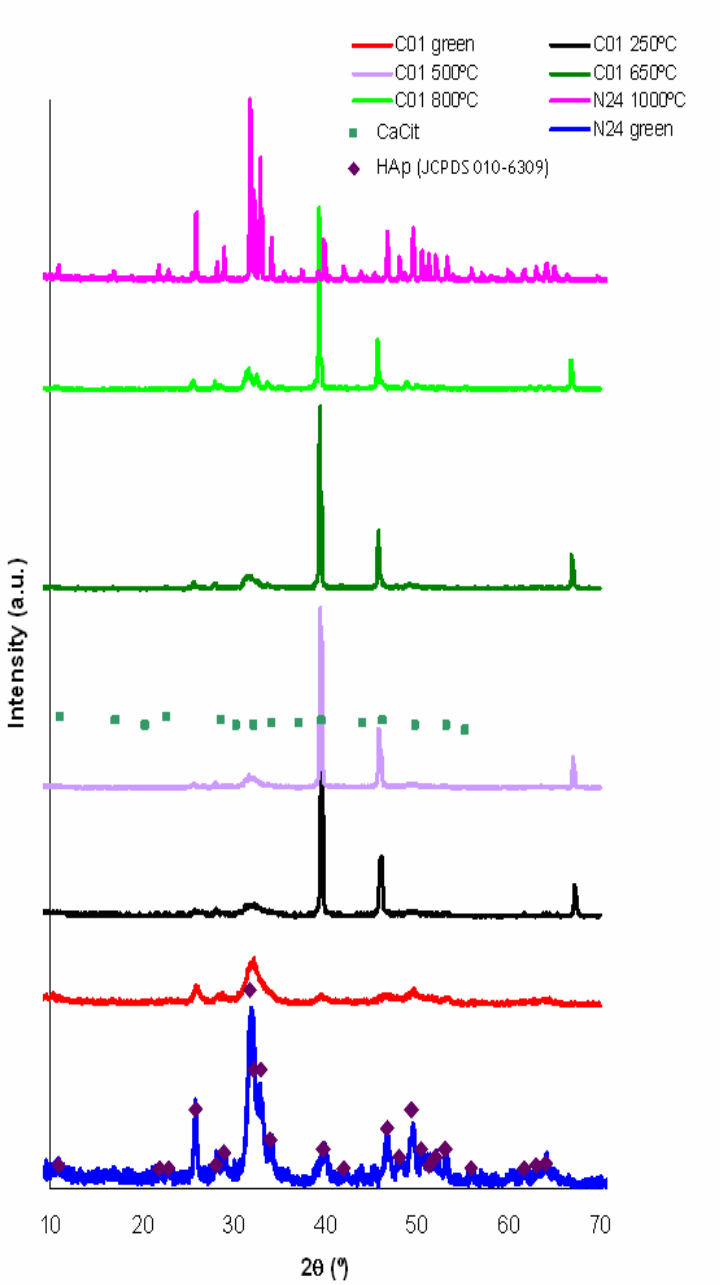

Figure 15. Evolution of XRD with temperature (C01), comparing with HAp without surfactant (N24).

When Ca^{2+} is present in excess in the bulk solution, calcium citrate, ($Ca_3(C_6H_5O_7)_2 \cdot 4H_2O$), rapidly forms and precipitates (López-Macipe et al. 1998; Martins et al. 2008; Misra 1996). To determine if precipitates and its amount, some calculations were made. In equilibrium, the constant of solubility product is defined as

$$Ksp = \left[C_6H_5O_7^{3-}\right]_{eq}^2 \left[Ca^{2+}\right]_{eq}^3 \quad (4)$$

According to Partheil and Hubner 1903 (see for example (Boulet and Marier 1960)), calcium citrate tetrahydrated solubility at 18ºC is $0.742 g/l\ (1.301 \times 10^{-3}\ mol.L^{-1})$ and thus

$$Ksp = (2s)^2 (3s)^3 = 108 s^5 \Leftrightarrow Ksp = 4.03 \times 10^{-13} \left(\frac{mol}{l} \right)^5 \quad (5)$$

where *Q* is the reaction quotient,

$$Q = \left[C_6 H_5 O_7^{3-} \right]^2 \left[Ca^{2+} \right]^3 \quad (6)$$

Comparing these two values, $Q > Ksp$, meaning that calcium citrate tetrahydrated, $Ca_3(C_6H_5O_7)_2 \cdot 4H_2O$, precipitates.

$$Ca_3(C_6H_5O_7)_2 \cdot 4H_2O(s) \longleftrightarrow 3Ca^{2+}(aq.) + 2C_6H_5O_7^{3-}(aq.) \quad (7)$$

In sample C02, the amount of calcium and citrate ions that reacted to form $Ca_3(C_6H_5O_7)_2 \cdot 4H_2O$ is about 15% and 33%, respectively.

However, (Boulet and Marier) say that crystals of calcium citrate only starts appearing after 2 days and agitation reduced this process. All the process of preparation of $CaCl_2$ and $K_3(C_6H_5O_7)_2$ was done under vigorous agitation reducing this tendency to precipitate. They also refer that in SEM images, calcium citrate tends to form clusters of needles, which was not observed in Figure 13.

The crystallite size was estimated from the X-ray diffractograms using the Scherrer formula (Martins et al. 2008)

$$D = \frac{k\lambda}{\beta_{1/2} \cos\theta} \quad (8)$$

D is the crystallite size (Å), *k* is a shape factor equal to 0.9, *λ* is the X-ray wavelength (1.54060 Å), *θ* is the diffraction angle and $\beta_{1/2}$ expressed in radians, is defined as

$$\beta_{1/2} = (B^2 - b^{2)^{1/2}} \quad (8)$$

Here *B* is the diffraction peak width at half height and *b* the natural width of the instrument related to the reflection plane [002]. The crystallite size of hydroxyapatite's green powder from sample C01 with 8 days of maturation is 17 nm, equation (7).

Some calculations were made, in order to compare this value with the obtained by a long run BET. The value obtained was 18.5 nm, which is close to the one calculated by equation (6) at 250ºC

Table 8. Surface area, Pore Volume and Pore Radius given by BJH method.

Surface area	157.218 m^2/g
Pore Volume	0.512 cc/g
Pore Radius (r)	95.342 A

Considering that all particles are spherical, with a smooth surface, the volume (V_{esf}) and surface area (S_{esf}) of a sphere are defined as

$$V_{esf} = \frac{4}{3}\pi r_p^3 (m^3) \tag{9}$$

$$S_{esf} = \frac{4\pi r_p^2}{1g}(m^2/g) \tag{10}$$

$$V_{esf} = \frac{m}{\rho_{ap}} \tag{11}$$

where ρ_{ap} is the apparent density, that is the mass per unit volume of a material, including the voids which are inherent in the material (12).

Dividing equation (9) by (8) and substituting V_{esf} (10):

$$\frac{S_{esf}}{V_{esf}} = \frac{\frac{4\pi r_p^2}{g}}{\rho_{ap} \times \frac{4}{3} \times \pi r_p^3} \rightarrow d_p = \frac{6}{S\rho_{ap}} \tag{12}$$

The apparent density is related to the porosity of the material ε_{ap} that represents the void spaces

$$\rho_{ap} = (1 - \varepsilon_{ap})\rho_s \tag{13}$$

$$\varepsilon_{ap} = \frac{V_p \rho_s}{1 + V_p \rho_s} \tag{14}$$

where V_p is the pore volume and ρ_s is the solid density.

Table 9. Values of solid density and apparent density.

ρ_s (g/m^3)	3.16x10^6
ρ_{ap} (g/m^3)	1.20x10^6

Differential scanning calorimetry was performed to the pure reactant, potassium citrate and to the washed gel sample C013. The potassium citrate sample presents two peaks, the first at 253.9ºC corresponding to dehydration and the second one at 279.1ºC corresponding to the melting point Figure 16 a). For the C013 sample one peak is observed at 140.9ºC that may correspond to the loss of all water, but there are no visible peaks around 279ºC. It is however important to refer that the reactant was in the form of powder and C013 in the form of gel. So, in the first case, all the mass introduced is dry reactant (powder) and in the case of C013 gel, 99% of the mass introduced, is water and only 1% is HAp, being almost imperceptible. Amplifying DSC signal between 210 and 300ºC, it is visible a weight loss Figure 16 b).

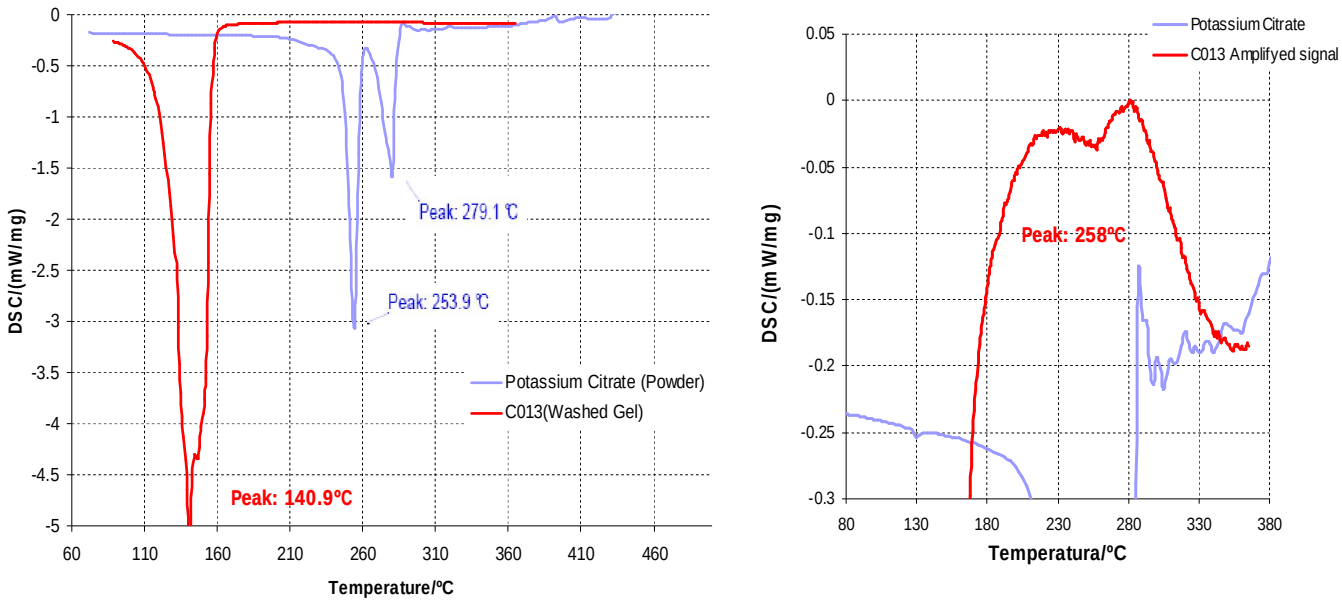

a) b)

Figure 16. Differential Scanning Calorimetry: a) pure reactant (potassium citrate) and washed gel of C01; b) potassium citrate and C013 amplified signal.

Observation of Figure 17, between 150 and 600ºC, shows a weight loss of about 18%. Around 90ºC both samples starts dehydrating, loosing physically absorbed water. Comparing both curves, they differ at about 270ºC. At this point, citrate starts melting, followed by citrate degradation and loss of chemical water.

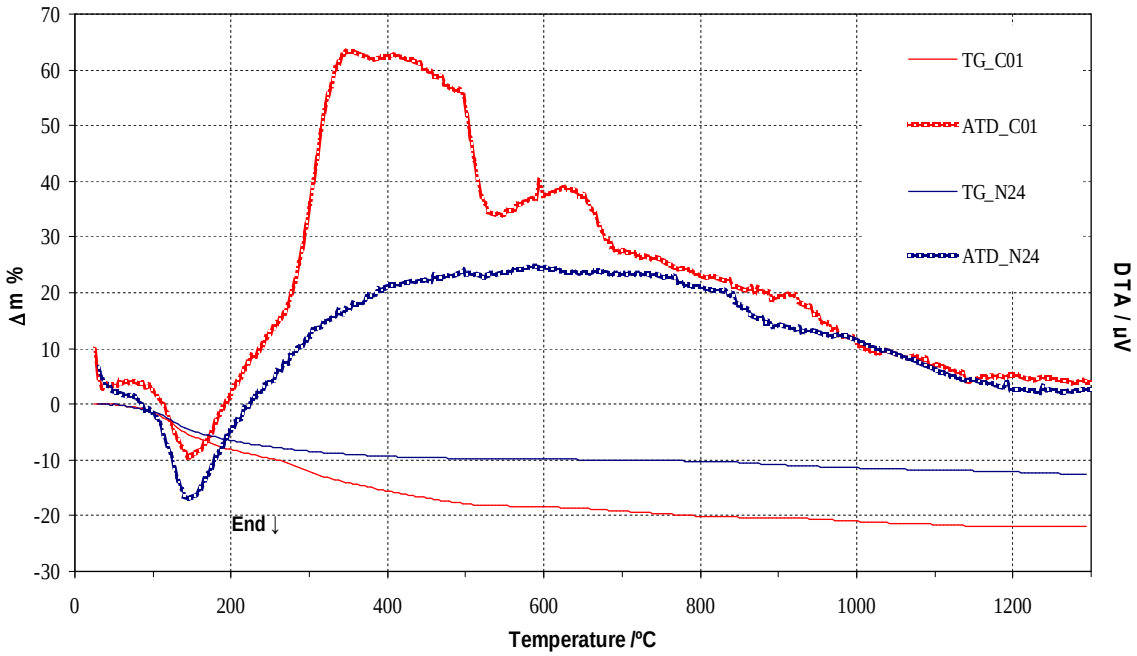

Figure 17. Thermogravimetric and differential thermal analysis (TG-DTA) for the C01 sample with 24h of aging (red) and sample N24 (blue).

4.4 Identification of functional groups

To obtain more information on the phases and other components of the synthesis gel, Fourier transform infrared spectroscopy (FT-IR) was used. B1, a commercial sample was analysed as well as two other samples without surfactant, N3 and N24. FT-IR spectra shown in Figure 18 for HAp powders, N3, N24, B1 and C013 gel, confirm the formation of hydroxyapatite apatite with the observed fundamental vibrational modes of PO_4^{3-} groups.

For sample C013 these are observed at 1081 and 908.4cm^{-1}. For the remaining samples there are additional frequencies at 1068 cm^{-1}, 1024–1036 cm^{-1} and 555–558 cm^{-1}. The band at 2700-3700 cm^{-1} derived from stretching vibration of hydrogen bonded OH groups in HAp.

Additionally, in C013 there are two peaks corresponding to a antisymmetric stretching vibration from the carboxylate group (COO^-) observed at 1602cm^{-1} and 1448cm^{-1} (Heese et al. 2008). These are wider and stronger than those for the HAp powders prepared without the addition of citrate.

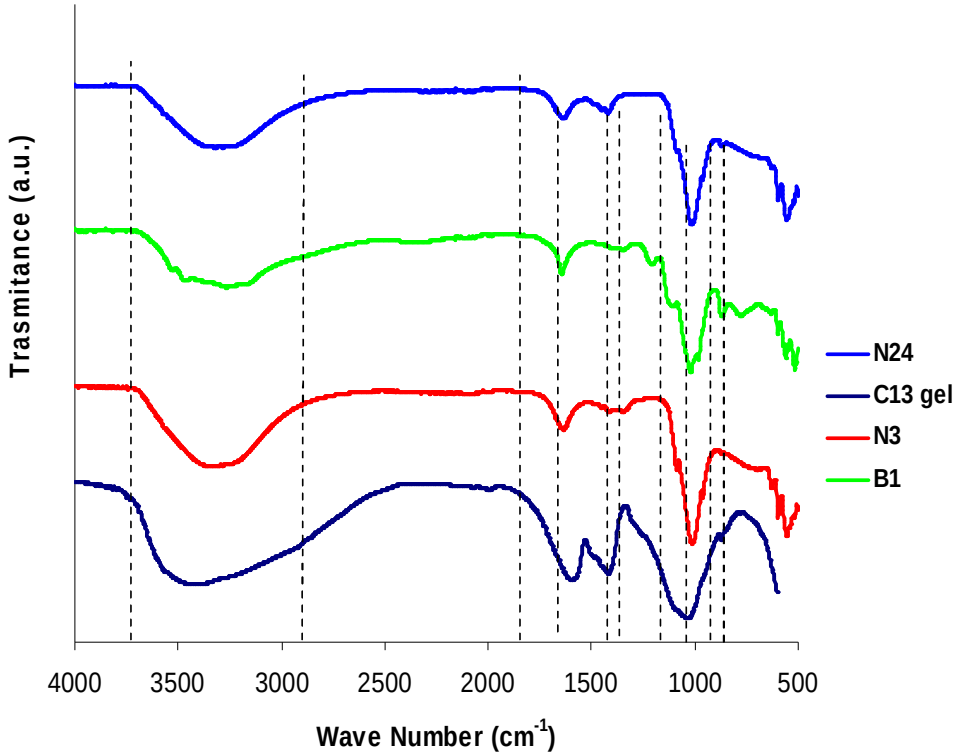

Figure 18. IR spectra of HAp of samples of HAp without surfactant (N3 and N24) and a commercial Sample (B1) with the produced sample of HAp with surfactant (C13).

4.5 Surface specific area (SSA)

The results shown in Figure 19 confirm the high surface area values expected. These are much higher than those referred in literature, due to the Hap's nanoparticles characteristics. It was noticed that the BET surface area differs on the ratio surfactant/calcium in a non linear relation.

Ratio Cit/Ca	SSA(m^2/g)
0.0015α	145.3
0.2000 α	305.3
0.9800 α	265.2
1.7400 α	245.1

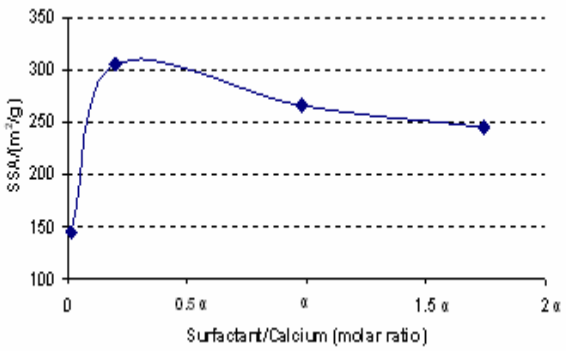

Figure 19. Evolution of the surface specific area with different molar ratio of surfactant/calcium.

Along the maturation step a decrease is observed (Figure 20), followed by an increase of the surface area, being that, at the end of 8 days, the surface area is higher than at the end of 1 day. This is due to the non-agglomeration of the particles. To understand this better, the reported value of sample N24 is 121 m^2/g.

Sample	Tempo (days)	SSA(m^2/g)
C01	1	220.1
	4	182.5
	8	265.2

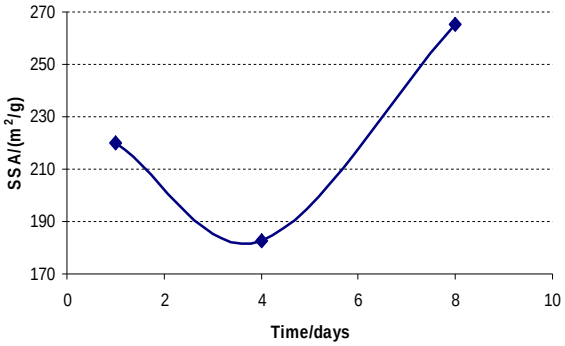

Figure 20. Evolution of the surface specific area along maturation.

5 Final Remarks

5.1 Conclusions

This work was designed to study the effect of the incorporation of surfactants to diffuse hydroxyapatite nanoparticles.

The goal was accomplished. Nanoparticles were dispersed in the suspension as it was shown by all the characterization analysis. The particle size distribution indicates an average distribution around 100 nm, but SEM images indicate a homogeneous size and an average diameter below 50 nm. The citrate (surfactant) concentration was found to have a great influence on nanoparticles surface area, the agglomeration state as well the physical state (in a transparent gel form). At a ratio surfactant/Calcium 0.2, HAp nanoparticles showed the highest surface area of 305 m2/g. The general particles morphology is rather regular. They have spherical shape with crystal size indicated by Sherrer formula of 17 nm and by BET analysis 18.5 nm. Looking for the high surface area values and the ability of the HAp nanoparticles being biocompatible, this product could be used for drug delivery in biomedical and cosmetic applications.

The maturation stage is necessary to balance ionic charges and for diffusing the particles. It also depends on the molar ratio used for surfactant/calcium amounts. To determine this ratio, calculations were made, considering the adsorption mechanism in a monolayer, on a 40 nm crystal.

XRD and DSC / TG-DTA requires further analysis (see future work) to investigate the thermo-kinetic applied in order to understand its mechanism. However due to the absence of any evidence of other elements in the XRD sample, only HAp was detected.

Additionally other tests as FTIR and EDS were performed. They confirm the existence of carbon in the sample, attributable to carboxylate group (COO^-) and their fine dispersion in the surface. Precipitation calculations were made, and the chosen surfactant, citrate, may precipitate with calcium, forming calcium citrate tetrahydrated. However, literature refers that agitation reduces its formation and the formation of needle-shape clusters. In the samples analysed, no such morphology was observed.

Though in case of calcium citrate's presence in the final product is not yet determined, calcium citrate is an approved compound by the FDA (Food and Drug Administration), and citrate is present in bone inorganic phase.

5.2 Other Activities

Along the duration of this work, there has been a direct guidance and a constant learning period; in the beginning, several laboratorial procedures were taught and also organizational and stock managing skills. These were all important procedures because they were the means to get more comfortable with all laboratory and analysis equipment. Together with this, all experiments were closely followed to better understand the influence of several parameters and conditions that influence the reaction's product quality, such as injection schemes, reactants and flowing regimes.

The first project I was involved was the PCM microcapsules production using the NETmix® reactor. It was a delicate but successful process.

Afterwards, several HAp experiments were conduced. The objective was to test some parameters and to learn in a more detailed way the process itself. After this, in parallel with other projects, series of experimental runs were done which marked this thesis subject start.

It was also given the opportunity to be part of the industrial NanoXIM•HAp70 commission unit. NanoXIM•HAp70 is a high purity product and has some unique properties. It is a hydroxyapatite tailor-made production, where the particles size and morphology, surface area and crystallinity are programmed to ensure the costumer needs and applications; it is one of Fluidinova's competitive advantages, possibly due to the versatility of the NETmix® technology. The first task was to ensure quality control of the industrial unit, and latter costumer's needs, by trying to produce a tailor-made product.

The latest NETmix® project I was able to contact with was the metallic nanoparticles production, as part of one Fluidinova's R&D project.

Simultaneously with all the experiments, background work of washing, centrifugation and posterior milling of the products obtained was carried out. These processes were always necessary to proceed to subsequent characterization of the product. Some of the characterization methods used in Fluidinova are Malvern and BET, to determine the particle's size distribution and its specific surface area, respectively. Several other analysis methods were outsourced such as DSC, TG-DTA, SEM, TEM and XRD. However, all sample preparation and result analysis were closely followed by me.

While working at Fluidinova, I had also the opportunity to be one of its representatives in the International Exhibition for the Construction Industry - Concreta, in the area of consulting services in industry, buildings and environment, using CFD. Although it was not directly related with this work, the experience permitted me to better understand the company's vision and its business areas and clients.

Apart from all the work, team spirit and help were a marking point.

5.3 Future Work

The initial expectations for this work were accomplished. The obtained product is a transparent gel, composed by nanoparticles well dispersed. However, further investigation is needed in order to obtain more information from all the techniques applied.

Additionally there is a need for more tests to optimize the citrate/calcium ratios and to do so, requires a deeper study on the adsorption mechanism of the surfactant. A different injection scheme should be tested in order to avoid possible calcium citrate precipitation.

Afterwards, when the mechanism and the process are fully comprehended, a scale up of the project for cosmetic applications may be done. A goal for future joint venture for developing a new product in the cosmetic field between Fluidinova and other cosmetic developer company is possible.

5.4 Final Appreciation

The work done throughout this thesis was very rewarding, since I had access to Fluidinova's know-how and I was allowed to develop technical knowledge and to assist in several areas of characterization and quality control of the final product.

Characterization of HAp nanoparticles allowed me to work with several equipments such as a Malvern to determine the distribution of particle size and BET to determine specific surface area (SSA), DSC and TG-DTA to observe the transition of phases and decomposition. I also acquired sensibility of interpretation of several other techniques as SEM, TEM, XRD and ICP.

This traineeship ensured a fertile environment for collaborative research that transcended traditional disciplinary boundaries. It was an environment full of diversity and our participation contributed to a broadly inclusive preparation, a globally engaged science and engineering workforce. I was able to observe the construction and startup of NanoXIM industrial unit, which was an exceptional experience.

6 References

Amjad, Z. (1987). "The Influence of Polyphosphates, Phosphonates, and Poly(carboxylic acids) on the Crystal Growth of Hydroxyapatite." *Langmuir*, 3, 1063-1069.

Balasundaramm, G., and Webster, T. J. (2006). "A perspective on nanophase materials for orthopedic implant applications." *J. Mater. Chem.*, 16, 3737-3745.

Bell, S. J. D. (2006). "Therapeutic Calcium Phosphate Particles in Use For Aesthetic or Cosmetic Medicine, and Methods of Manufacture and Use." W. I. P. Organization, ed., U.S.

Botelho, C. M. d. C. F. (2005). "Silicon-substituded hydroxyapatite for biomedical applications," Oporto

Boulet, M., and Marier, J. R. (1960) "Solubility of Tricalcium Citrate in Solutions of Variable Ionic Strength and Milk Ultrafiltrates."

Byrappa, B. (2003). "Crystal Growth Technology." *William Andrew Publishing/Noyes*.

Chan, C. K., Kumar, T. S., Liao, S., Murugan, R., Ngiam, M., and Ramakrishnan, S. (2006). "Biomimetic nanocomposites for bone graft applications." *Nanomedicine*, 1, 177-188.

Chen, C.-W., Riman, R. E., TenHuisen, K. S., and Brown, K. (2004). "Mechanochemical–hydrothermal synthesis of hydroxyapatite from nonionic surfactant emulsion precursors." *Journal of Crystal Growth*, 270, 615-623.

Dorozhkin, S. V., and Epple, M. (2002). "Biological and Medical Significance of Calcium Phosphates." *Angew. Chem. Int.*, 41, 3130 - 3146.

Feng, W., Mu-sen, L., Yu-peng, L., and Young-xin, Q. (2005). "A simple sol-gel technique for preparing hydroxyapatite nanopowders." *Materials Letters*, 59, 916-191.

Fluidinova. www.fluidinova.pt.

Ginebra, M. P., Traykova, T., and Planell, J. A. (2006). "Calcium phosphate cements as bone drug delivery systems: A review

" *Journal of Controlled Release*, 113, 102-110.

Gomes, P. J., Silva, V. M. T. M., Quadros, P. A., Dias, M. M., and Lopes, J. C. B. (2007). "A Highly Reproducible Continuous Process for Hydroxyapatite Nanoparticles Synthesis."

Gómez-Morales, J., Torrent-Burgués, J., and Rodríguez-Clemente, R. (2001). "Continuous precipitation of hydroxyapatite from Ca/citrate/phosphate solutions using microwave heating " *Cryst. Res. Technol* 36, 1065.

Heese, M., Meier, H., and Zeeh, B. (2008). *Spectroscopy Methods in Organic Chemistry*, Thieme.

Itatani, K., Iwafune, K., Howell, F. S., and Aizawa, M. (1999). "Preparation of various calcium phospate powders by ultrasonic spray freeze-drying technique." *Materials Research Bulletin*, 35, 575-585.

Kandori, K., Fudo, A., and Ishikawa, T. (2002). "Study on the particle texture dependence of protein adsorption by using synthetic micrometer-sized calcium hydroxyapatite particles." *Colloids and Surfaces B: Biointerfaces* 24 145-153.

Koutsopoulos, S. (2002). "Synthesis and characterization of hydroxyapatite crystals: A review study on the analytical methods." Department of Chemistry, University of Patras.

Kwon, S.-H., Jun, Y.-K., Hong, S.-H., and Kim, H.-E. (2003). "Synthesis and dissolution behavior of b-TCP and HA/b-TCP composite powders." *Journal of the European Ceramic Society*, 23, 1039-1045.

Laranjeira, P. E. M. S. C. (2005). "NETMIX Static Mixer Modelling, CFD Simulation and Experimental Characterisation," Faculdade de Engenharia Universidade do Porto.

Leventouri, T. (2006). "Synthetic and biological hydroxyapatites: Crystal structure questions." *Biomaterials*, 27, 3339-3342.

Li, B., Wang, X. L., Guo, B., Xiau, Y. M., Fan, H. S., and Zhang, X. D. (2007a). "Preparation and Characterization of Nano Hydroxyapatite." *Key Engineering Materials*, 330-332, 235-238.

Li, Y., Tjandra, W., and Tam, K. C. (2007b). "Synthesis and characterization of nanoporous hydroxyapatite using cationic surfactants as templates

" *Materials Research Bulletin*.

Lopes, J. C. B., Dias, M. M. Q., Silva, V. M. T. M., Santos, P. A. Q. O., Monteiro, F. J. M., P.J.C.Gomes, and Mateus, A. Y. P. (2006). "Método de produção de nanopartículas de fosfatos de cálcio com elevada pureza e respectiva utilização." Pedido.

López-Macipe, A., Gómez-Morales, J., and Rodr guez-Clemente, R. (1998). "The Role of pH in the Adsorption of Citrate Ions on Hydroxyapatite." *JOURNAL OF COLLOID AND INTERFACE SCIENCE*, 200, 114-120.

Lu, G. Q., and Zhao, X. S. "Nanoporous Materials - An Overview."

Manuel, C. M., Ferraz, M. P., and Monteiro, F. J. (2003). "Synthesis of Hydroxyapatite and Tricalcium Phosphate Nanoparticles-Preliminary Studies." *Key Engineering Materials*, 240-242, 555-558.

Martins, M. A., Santos, C., Almeida, M. M., and Costa, M. E. V. (2008). "Hydroxyapatite micro- and nanoparticles: Nucleation and growth mechanisms in the presence of citrate species." *Journal of Colloid and Interface Science* 318, 210-216.

Mastersizer2000. (2007). *User Manual*.

Misra, D. N. (1996). "Interaction of Citric Acid with Hydroxyapatite: Surface Exchange of Ions and Precipitation of Calcium Citrate." *J Dent Res.*, 75, 1418-1425.

Murugan, R., and Ramakrishna, S. (2005). "Development of nanocomposites for bone grafting." *Composites Science and Technology*, 65, 2385-2406.

Netzsch. "www.netzsch-thermal-analysis.com."

Onuama, K., and Ito, A. (1998). "Cluster Growth Model for Hydroxyapatite." *Chem. Mater.*, 10, 3346-3351.

Pradeesh, T. S., Sunny, M. C., Varma, H. K., and Ramesh, P. (2005). "Preparation of microstructured hydroxyapatite microspheres using oil in water emulsions." *Bull. Mater. Sci.*, 28, 383-390.

Quantachrom, I. *Quantachrom Nova 2000e user manual*.

Rangavittal, N., Landa-Cánovas, A. R., González-Calbet, J. M., and Vallet-Regí, M. "Structural study and stability of hydroxyapatite and b-tricalcium phosphate: Two important bioceramics."

Rauschmann, M. A., Wichelhaus, T. A., Stirnal, V., Dingeldein, E., Zichner, L., Schnettler, R., and Alt, V. (2005). "Nanocrystalline hydroxyaptatite and calcium suiphate as biodegradable composite carrier material for local delivery of antibiotics in bone infections." *Biomaterials*, 26, 2677-2684.

Rodríguez-Lorenzo, L. M., Vallet-Reg, M., and Ferreira, J. M. F. (2001). "Colloidal processing of hydroxyapatite " *Biomaterials*, 22, 1847-1852.

Sikirić, M. D., and Füredi-Milhofer, H. (2006). "The influence of surface active molecules on the crystallization of biominerals in solution

" *Advances in Colloid and Interface Science*, 128-130, 135-158.

Silva, V. M. T. M., Quadros, P. A., Laranjeira, P. E. M. S. C., Dias, M. M., and Lopes, J. C. B. (2008). "A novel continuous industrial process for producing hydroxyapatite nanoparticles."

Thamaraiselvi, T. V., and Rajeswari, S. (2004). "Biological Evaluation of Bioceramic Materials - A Review." *Trends Biomater. Artif. Organs*, 18 (1), 9-17.

Torrent-Burgues, J., and Rodriguez-Clemente, R. (2001). "Hydroxyapatite Precipitation in a Semibatch Process." *Cryst. Res. Technol.* , 36, 1075-1082.

Vallet-Regí, M., and González-Calbet, J. M. (2004). "Calcium phosphates as substitution of bone tissues." *Progress in Solid State Chemistry*, 32 1-31.

Vallet-Regía, M., and González-Calbet, J. M. (2004). "Calcium phosphates as substitution of bone tissues." *Progress in Solid State Chemistry*, 32 1-31.

Wang, Y., Chen, J., Wei, K., Zhang, S., and Wang, X. (2006). "Surfactant-assisted synthesis of hydroxyapatite particles." *Materials Letters*, 60, 3227-3231.

Wu, Y., and Bose, S. (2005). "Nanocrystalline Hydroxyapatite: Micelle Templated Synthesis and Characterization." *Langmuir*, 21, 3232-3234.

Yao, J., Tjandra, W., Chen, Y. Z., Tam, K. C., Mab, J., and Soha, B. (2003). "Hydroxyapatite nanostructure material derived using cationic surfactant as a template." *J. Mater. Chem.*, 13, 3053-3057.

Yoshimura, M., and Suda, H. (1994). *Hydrothermal Processing of Hydroxyapatite:Part, Present and Future, in: Hydroxyapatite and Related Materials*, P. W. Brown and B. Constanz, eds.

7 Appendices

Appendix A – Cristallographic Calculation

A unit cell consists of two triangular prismatic subcells (Figure 21), constituted by ten calcium atoms, three phosphoric groups and two hydroxide groups.

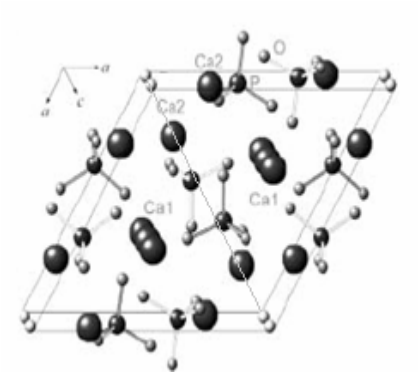

Figure 21. Unit cell of hydroxyapatite.

These calculations intended to determine the amount of external calcium that could adsorbe citrate, considering a crystal growth of 40nm. From the total amount of calcium atoms in the structure (10 calcium atoms), only 6 of them are considered as external ions: 2 $Ca(1)$ and 4 $Ca(2)$.

As it was previously said, the hexagonal structure of HAp is composed by three unit cells (*Figure 1*). Although the total number of calcium ions grows with this aggregation, the number of external calcium atoms does not increase equally.

In the crystal, parts of calcium atoms are shared with the nearby unit cells (4 $Ca(2)$). From the 42 calcium atoms [$Ca_{atoms} = 10Ca \times 3c.u. + 4Ca(2) \times 3c.u.$] only 24 are external. A cluster will grow by aggregation of small crystals. Although no definite cluster grow is known (only by simulation (Onuama and Ito 1998)), it was considered the cluster would grow in an organized way, by adding crystals in all available faces. So, the calculations were done considering that there are 3 external calcium atoms in the superior face and 1 external calcium atom in the lateral face.

In one layer (Figure 22) there are 21 crystals [$Crystal_{1layer} = (1+6) \times 3$] and 630 total calcium atoms, from which only 192 can adsorbe.

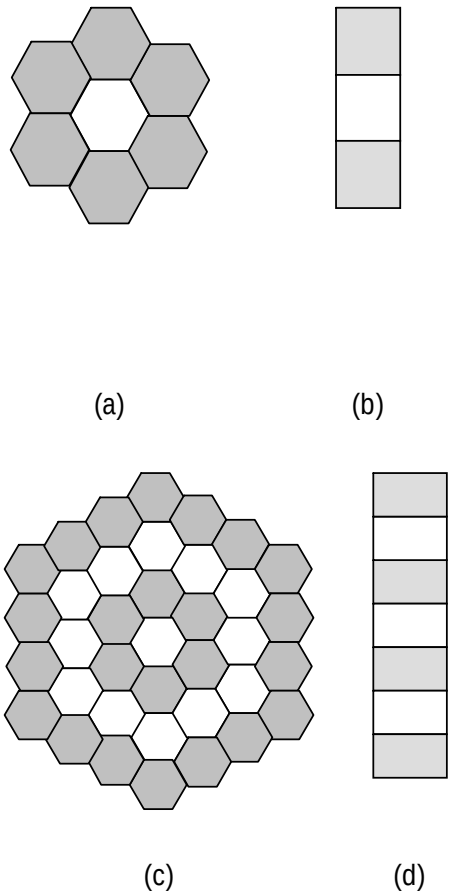

Figure 22. .(a) and (b): upper and side view of a one layered crystal, respectively;(c) and (d): upper and side view of a crystal with three layers, respectively.

In the final calculations, to the total calcium atoms must be added the corresponding external atoms half parts.

Appendix B – Washing Procedures

The washing procedure was a demanding work, due to the need to stop the maturation stage. For all fourteen experiments done, suspensions were washed at the end of 1hour, 24 hours, 4days, 7 days and 30 days. Since HAp nanoparticles in suspension were completely dispersed, large centrifugation times were needed.

In each centrifuge flask 255g of suspension was introduced and pH and conductivity values were controlled.

Table 10. Time of centrifugation, gel weight, supernatant pH and conductivity for samples at different periods of maturation.

Sample C01	t_{cent} (min)	w_{gel} (g)	$pH_{sobren.}$	$\Lambda_{sobren.}$ (mS/cm)
1h	30	9.8	12.52	52.00
	45	9.5	12.50	51.90
	90	9.3	11.07	1.19
	120	9.1	10.28	0.14
24h	30	25.3	12.44	52.20
	45	24.9	11.46	5.42
	90	20.2	10.82	0.95
	120	20.0	10.70	0.35
4 days	120	3.9	12.45	55.30
	240	3.2	11.41	29.30
	240	3.8	10.63	0.09
7 days	120	3.0	12.25	55.30
	240	2.8	11.20	19.30
	240	2.3	10.48	0.55
30 days	120	3.1	11.96	65.00
	240	2.8	10.80	1.00
	240	2.2	9.44	0.03

Appendix C – Ball Mill Operating Conditions

This operation was performed in a Planetary ball mill. The real grinding bowl capacity is 250ml, but the useful capacity is 162.5ml (Table 11).

Table 11. Ball Mill capacity

Real capacity (ml)	250,0
Useful capacity (ml)	162,5

Table 12. Amount of used balls.

Balls	Amount
Small balls	30
Average balls	12
Big balls	2

Table 13. Unit agate balls capacities

Balls	Occupied Volume (ml)
Small balls	0,5236
Average balls	4,1888
Big balls	14,1372

Table 14. Operating conditions.

Milling time (min):	60
Rotation speed (rpm):	200
Milling break (min):	5 min/(break:4s)
Inversion (Y/N):	Yes

Appendix D - Suspensions Photographs

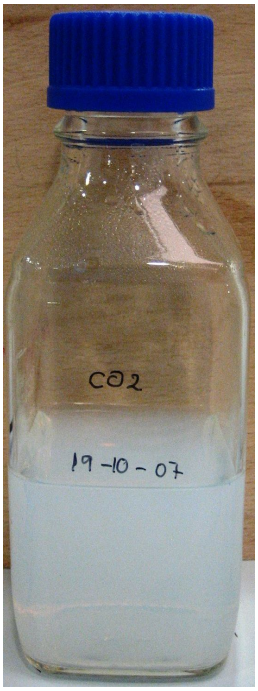

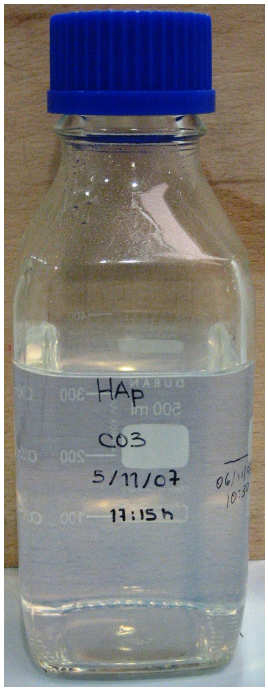

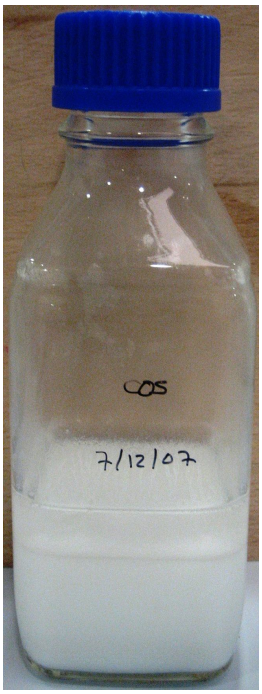

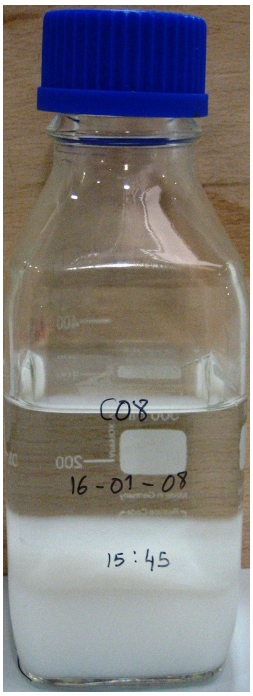

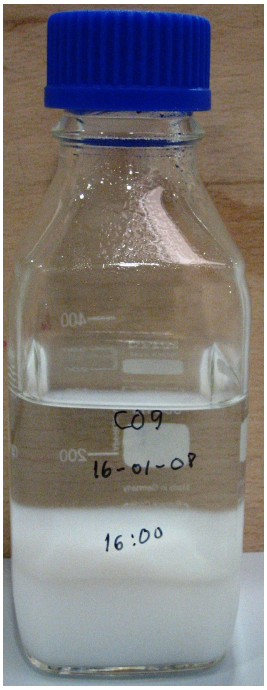
C09
16-01-08
16:00

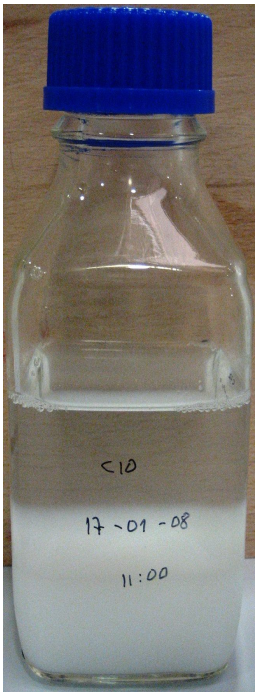
C10
17-01-08
11:00


C11
16-01-08
14:20


C12
17/01/08
11:30


C13
17-01-08
12:15


C014
23-01-08
16:30

Appendix E – Hydroxyapatite Synthesis Methods

Table 15. Preparation Techniques for Hydroxyapatite. Adapted from (Yoshimura and Suda 1994).

Techniques	Starting Materials	Synthetic Conditions	Comments
Solid State Reaction	$Ca_3(PO_4)_2 + CaCO_3$ $Ca_2P_2O_7 + CaCO_3$	900-1300°C, usually with water vapor	Ca/P-1.67, large grain size, irregular forms, inhomogeneous flowing
Wet Chemical Method	$Ca(NO_3)_2 + (NH_4)_2 HPO_4$ $Ca(OH)_2 + H_3PO_4$	R.T.-100°C pH: 7-12	Ca/P < 1.67 fine irregular crystals with low crysatllinity inhomogeneous
Hydro-Thermal Method	wet chemically prepared HAp, other calcium phosphates, seeding	100-200°C (1-2 MPa), 300-600°C (1-2 Kbar)	Ca/P=1.67 homo-geneous, fine single crystals or large crystals
Gel Growth Method	Gel + Ca^{2+} + PO_4^{3-}	R.T.-60°C, pH: 7-10	large Monetite, Brushite, OCP, but small HAp
Flux Growth Method	CaF_2, $CaCl_2$ as flux $Ca(OH)_2$ as flux	1325°C (FAp,ClAp) HAp	large crystals with little lattice strain